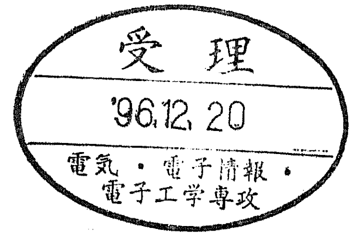

子 344

Fabrication of Quantum Wires by Metalorganic Chemical Vapor Selective Deposition and Applications to Opto-electronic Devices

(有機金属気相選択成長による量子細線の作製と光デバイスへの応用)

A Thesis Presented to the Graduate School of the University of Tokyo
in Partial Fulfillment of the Requirements
for the Degree of Doctor of Philosophy in Electronic Engineering

by

Taro Arakawa

December 20, 1996

To My Parents

Preface

This thesis describes an essential part of the research carried out at Institute of Industrial Science, University of Tokyo, under the supervision of Professor Yasuhiko Arakawa while the author was working as a graduate student of the Department of Electronic Engineering, University of Tokyo, from 1992 to 1997.

For future applications of quantum nanostructures such as quantum wires and quantum dots to opto-electronic devices, developments of fabrication technologies of the quantum nanostructures and research of their optical and electronic properties. At the present stage, since the fabrication technologies of the quantum wires and dots are not sufficiently developed, the device applications as actual products are limited within the quantum well devices.

In this thesis, the author describes fabrication of quantum wires by metalorganic chemical vapor selective deposition and applications to opto-electronic devices.

December 1996 *Taro Arakawa*

Acknowledgments

The author would like to express his sincere gratitude to his dissertation supervisor, Professor Yasuhiko Arakawa, Institute of Industrial Science, University of Tokyo, for his constant guidance, enthusiasm, and encouragement throughout my graduate studies at University of Tokyo. His suggestions were always full of insight, and he showed the author what the "research" in the university was. Without them, this work could be accomplished.

The author would like to thank Professor H. Sakaki, Institute of Industrial Science, University of Tokyo, Professor T. Ikoma, Institute of Industrial Science, University of Tokyo, and Associate Professor K. Hirakawa, Institute of Industrial Science, University of Tokyo, for their encouragement and experimental supports.

The author wishes to express his thanks to Professor Y. Fujii, Institute of Industrial Science, University of Tokyo (at present, Nippon University), Associate Professor T. Hiramoto, Institute of Industrial Science, University of Tokyo, and Associate Professor T. Takahashi, Research Center for Advanced Science and Technology, University of Tokyo, for their kind encouragement.

The author would like to thank his thesis committee, Professor K. Tada, University of Tokyo, Professor H. Sakaki, Institute of Industrial Science, University of Tokyo, Professor K. Kamiya, University of Tokyo, Associate Professor K. Hirakawa, Institute of Industrial Science, University of Tokyo.

The author wishes to express his appreciation to Mr. M. Nishioka, Research Associate, Institute of Industrial Science, University of Tokyo, and Mr. S. Ishida, Technical Associate, Institute of Industrial Science, University of Tokyo, who were his co-workers, and whose technical assistance in the experimental aspects of this thesis and discussion were invaluable.

The author would like to thank Miss K. Arai, Mrs. N. Kaya, Miss Y. Fujioka, and Mrs. I. Fukatsu, Secretaries, who provided faithful assistance for his research

The author would like to thank Dr. S. Tsukamoto, National Research Institute for Metal, Science and Technology Agency, for his guidance, fruitful discussion, constant encouragement.

The author would also like to thank Dr. T. Noda, Institute of Industrial Science, University of Tokyo, Mr. Y. Shimada, Institute of Industrial Science, University of Tokyo, and Dr. Y. Nagamune, Electrotechnical Laboratories, for their discussions, encouragement, and technical supports.

The author is grateful to Dr. F. Sogawa for his fruitful discussion, help in optical measurements. The author is indebted to Dr. Y. Toda for PL measurements with near-field scanning optical microscope. The author is also indebted to Mr. Y. Kato for his collaboration in works on quantum confined Stark effect. The author wishes to thank Mr. L. Finger for his collaboration in PLE measurements. The author is grateful to Mr. H. Watabe, Mr. K. Suzuki and Mr. H. Hayashi for their technical assistance in micro-PL measurements. The author would like to thank Mr. M. Kitamura for his collaboration in the experiments in QCSE measurements.

The author would like to express his gratitude to Dr. K. Wada, NTT, for CL measurements.

The author wishes to express his appreciation to many other colleagues, Dr. Z. L. Zhang, Dr. X. P. Feng (University of Melobourn), Dr. J. Oshinowo (Universitat Wurzburg), Dr. J. H. Lee (Electronics and Telecommunications Research Institute), Dr. T. Tanaka (Fujitsu), Mr. S. Nakayama (Sony), Mr. R. Schur, Mr. S. Shinomori, Mr. Matsuda, Mr. M. Nielsen, Dr. Lee, Dr. T. Someya, Mr. Narihiro, Mr. N. Sekine, Mr. M. Endo (Sony), for their kind and valuable cooperation and collaborations.

The author would like to thank Mr. S. Matsumoto, University of Tsukuba, for his assistance in the experiments. The author wishes to thank Mr. T. Kono (Mitsubishi Electric) for his encouragement in his graduate school days.

The author also gratefully acknowledges the financial support of the University-Industry Joint Project on "Quantum Nanoelectronics", a Grant-in-Aid for Scientific Research on Priority Areas "Quantum Coherent Electronics", supported by the Ministry of Education, Science and Culture. The fellowship of the Japan Society for the Promotion of Science for Japanese Junior Scientists was generously supplied from 1994 April to 1997 March.

Finally, the author would like to express his sincere gratitude to his parents, Fuji and Fujiko for their constant encouragement and hearty support.

Abstract

The author has established the understanding of quantum wires from the view points of both fabrication technologies and applications to optical devices. In this study, the author focused on the following two subjects particularly.

1) Fundamental study of fabrication technologies for quantum wires and their optical properties.

2) Applications of quantum wires to optical devices such as lasers and optical modulators.

With respect to 1), optical properties of V-groove shaped GaAs and InGaAs quantum wires are discussed. Fabrication technique for ridge-type InGaAs quantum wires on a (110) cleaved facet are developed as a fundamental technology for fabrication of quantum wire structures.

With respect to 2), fabrication and optical properties of microcavity quantum wire lasers are investigated. The quantum confined Stark effect in quantum wires is also discussed as a fundamental study for optical modulators.

Contents

Preface iii
Acknowledgments iv
Abstract vii
Contents viii

Chapter 1 Introduction 1

1.1 Background of This study 1
1.1.1 Fabrication technologies of quantum wire structures 1
1.1.2 Application of quantum wires to optoelectronic devices 4
1.2 Motivation and Objectives of This Study 5
1.3 Synopses of This Thesis 7

Chapter 2 Fabrication and Optical Properties of GaAs and InGaAs Triangular-Shaped Quantum Wires 9

2.1 Introduction 9
2.2 Fabrication Process of Triangular-Shaped Quantum Wire Structures 12
2.3 Optical Properties of GaAs and InGaAs Quantum Wires 14
2.3.1 Photoluminescence at low temperature 14
2.3.2 Temperature dependence of photoluminescence 17
2.3.3 Photoluminescence excitation measurements 20

2.3.4 Photoluminescence observation with near-field scanning optical microscopy 23
2.3.5 Cathodoluminescence measurements 25
2.4 Concluding Remarks 27

Chapter 3 Fabrication and Optical Properties of InGaAs Quantum Wires Grown on a (110) Cleaved Plane of AlGaAs/GaAs Superlattice 44

3.1 Introduction 44
3.2 Fabrication of the quantum wire structures 46
3.2.1 Fabrication process 46
3.2.2 Native oxide layer on AlxGa1-xAs 47
3.2.3 Growth behavior of InGaAs on a (110) Plane 49
3.2.4 Growth condition and grown structure 50
3.3 Photoluminescence Measurements 51
3.4 Spatially Resolved Photoluminescence Measurements 53
3.5 Concluding Remarks 54

Chapter 4 Fabrication of Microcavity Quantum Wire Lasers 63

4.1 Introduction 63
4.2 Fabrication of Microcavity Laser Structures 65
4.2.1 Fabrication process of 4λ-microcavity lasers 65
4.2.2 Fabrication process of 2λ-microcavity lasers 67

4.3 Optical Characteristics of Microcavity Lasers 69
4.3.1 Photoluminescence of AlGaAs/InGaAs/GaAs quantum wires without a cavity 69
4.3.2 Photoluminescence of QWR laser structure with a cavity 70
4.3.3 Lasing characteristics of QWR lasers 71
4.4 Concluding Remarks 72

Chapter 5 Quantum Confined Stark Effect in GaAs Quantum Wires 82

5.1 Introduction 82
5.2 Sample Structure 84
5.3 Photoluminescence Measurements 85
5.4 Time Resolved Photoluminescence Measurements 90
5.5 Concluding Remarks 92

Chapter 6 Conclusion 102

Bibliography 106
Publication List 117

Chapter 1

Introduction

1.1 Background of This Study

1.1.1 Fabrication technologies of quantum wire structures

One dimensional and zero dimensional semiconductor structures receive great attention due to theoretically expected new physical properties which are interesting also for device applications. These one dimensional and zero dimensional structures are called quantum wires (QWRs) and quantum dots (QDs), respectively. Reduction of dimensionality of a system results in dramatic change for the energy dependence of the density of states which leads to modified optical and transport properties. For instance, quantum wires are expected to show unique electrical transport properties and to have extremely high electron mobilities[1]. In the optical device field, the QWR and QD heterostructures are expected to exhibit larger electro-absorption and electrorefraction[2], enhanced optical nonlinearities[3], and higher differential optical gain which leads to larger modulation bandwidth ,narrower linewidths[4], and higher characteristic temperature T_0[5], compared to more conventional semiconductors. In addition, the extremely small volume of inverted material and the higher gain in QWR lasers is expected to yield very low threshold currents, in the μA

-current regime. Therefore, considerable efforts have been devoted to fabrication and experimental investigation of these structures.

The remarkable developments in crystal growth technologies such as molecular beam epitaxy (MBE) and metalorganic chemical vapor deposition (MOCVD) have enabled the realization of the low dimensional semiconductor structures with high purity and sharp interfaces. In fact, quantum well lasers were realized, leading to improvements of laser parameters.

In order to realize these lower dimensional semiconductor structures, various approaches have been taken. In the following, we focus on fabrication of QWR structures. Conventional quantum well patterning techniques by reactive ion etching[6, 7], ion beam milling[8, 9] and wet chemical etching[10, 11], followed by epitaxial regrowth, result in imperfect quantum wire interfaces which is particularly detrimental for achieving high performance devices. In order to overcome these problems, growth technique using vicinal substrates[12-16], nonplanar substrates[17], and masked substrates[18-22] have also been investigated.

The growth technique of quantum wires on nonplanar substrates is one of the most promising. The advantages of this technique is as follows; the size and shape of the quantum wire can be controlled by the substrate pattern and/or growth conditions, damage-free interfaces can be obtained, vertically stacked structures can be formed, which increase the density of the quantum wires.

Selective growth (or selective area growth) techniques are also very promising for fabricating QWR and QD structures. Because of *in-situ* growth with self-alignment process of crystal facets, these method can produce QWR and QD structures of high uniformity and

damage free interfaces. The selective growth was applied for fabricating the QWR structures by using MOCVD selective growth in 1989 for the first time[23, 24]. Tsukamoto *et al.* developed the fabrication techniques of triangular shaped QWR structures by the MOCVD selective growth[25]. They obtained the QWRs of high quality.

In addition, a cleaved edge overgrowth method[26] recently receives attention. This method is capable of producing T-shaped quantum wires, proposed by Chan *et al*[27]. QWRs formed by this technique are very uniform[28, 29] and are suitable for characterization of physical properties of QWRs. However, lateral confinement is not sufficiently strong and it seems difficult to apply the QWRs to the actual devices at present.

As a unique method for formation of quantum wire structures, Notomi *et. al.* fabricated GaAs QWR structures using a selective growth technique on a cleaved facet of AlGaAs/GaAs superlattice by MOCVD[30]. Concerning this technique, we discuss in Chapter 3.

1.1.2 Applications of quantum wires to optoelectronic devices

Due to the advantages in QWRs as mentioned above, applications of QWR structures to electronic and optical devices, especially laser diodes, have been studied intensively. Focusing on actual laser diodes, the first semiconductor laser with QWR like active region was demonstrated in 1988 by Cao *et al*[31]. However, the device was operated only at low temperatures and with high threshold currents and no evidence for lateral quantum size effects was found in these devices. Various types of laser structures with QWRs have been investigated so far; GaAs/AlGaAs[32] and strained InGaAs/GaAs[33] QWR lasers grown on non-planar substrates, InGaAs/InGaAsP strained MQW lasers with Wire like active regions by chemical etching[34], GaAs QWR lasers using fractional layer superlattices[35, 36], GaAs/AlGaAs QWR lasers fabricated by cleaved edge overgrowth[37], QWRs by using vicinal substrates[38] and T-shaped GaAs QWR laser structure[28].

In spite of such intensive investigation, low threshold, ultra-high speed QWR lasers as predicted in theoretical analyses have not been realized so far. This is because it is still difficult to fabricate QWR structures of sufficiently high quality for bringing out their potential.

There are very few experimental reports on other optical devices such as modulators.

1.2 Motivation and Objectives of This Study

For future ultrafast optoelectronic systems such as optical information processing systems, high speed optical communication systems and so on, improvements of optical devices with quantum nanostructures such as QWRs and QDs are highly expected. To this goal, many works have been carried out as described in the previous section.

Though fabrication technologies for QWRs have not been fully established yet, our group has come to obtain rather good QWR structures by using the MOCVD selective growth technique. Hence, it is important to investigate optical properties of the QWRs from the view point of not only physics but application to actual devices. Strained QWRs are also very interesting because they are expected to give us further improvement in device performance.

On the other hand, despite of the intensive studies as described in the previous section, structural fluctuation in heterointerfaces is still the most serious problem in the nanostructures. In order to overcome this problem, it is necessary to investigate fabrication techniques from other angles.

In addition, it is important to study how promising the QWR structures are for application to actual optical devices.

The purpose of this study is to understand optical properties of GaAs and strained InGaAs QWR structures and proposal of a new method of fabrication of QWR structures, as a fundamental study for application of QWRs to actual devices.

Furthermore, feasibility of optical devices based on the QWR structures are studied. Therefore, QWR laser structures with a microcavity and the quantum confined Stark effect in QWRs have been demonstrated and investigated.

1.3 Synopses of This Thesis

In this thesis, fabrication of QWRs by metalorganic chemical vapor selective deposition and applications of QWRs to opto-electronic devices are investigated in order to realize high performance optical devices. This thesis is organized as follows:

In Chapter 1, the background of the present study is described with emphasis on fabrication of QWR structures. The aim of this thesis is also given.

In Chapters 2 and 3, fundamental studies of fabrication and optical properties of the QWR structures are described.

In Chapter 2, growth process of V groove shaped GaAs and strained InGaAs QWR structures are reviewed. Their optical properties are also discussed on the basis of photoluminescence, photoluminescence excitation measurements, and near-field scanning optical microscopy.

Chapter 3 describes the work on a new fabrication technique and micro-photoluminescence imaging of ridge-type InGaAs QWRs grown on a (110) cleaved plane of AlGaAs/GaAs superlattice. This technique was developed in order to overcome the limit of conventional lithography techniques.

In Chapters 4 and 5, applications of QWRs to optical devices are discussed.

Chapter 4 describes the work on fabrication of vertical-microcavity QWR lasers as a step toward the ultimate lasers on the basis of the established technology described in Chapter 2. Laser oscillation is demonstrated in a 4-λ cavity laser.

Chapter 5 describes photoluminescence studies of GaAs QWRs with quantum confined Stark effect. A clear blue shift of the photoluminescence peak based on enhanced exciton binding energy was observed with the increase of electric fields. Time-resolved PL measurements were also performed.

In Chapter 6, the conclusions of this work is given.

Chapter 2

Fabrication and Optical Properties of GaAs and InGaAs Triangular-Shaped Quantum Wires

2.1 Introduction

Low-dimensional semiconductor structures such as quantum wires have recently received great attention because new physical phenomena with possible applications to semiconductor lasers and other functional optical devices are expected[5, 39]. To fabricate these microstructures, selective growth on patterned substrates is one of the most attractive techniques[17, 20, 22, 25, 40]. QWR heterostructures suitable for optoelectronic applications need to meet a number of structural qualities. Formation of distinct quasi-1D subbands in the energy spectrum requires that the potential wells defining the wires be sufficiently narrow and uniform to yield subband separations $\Delta E > k_B T$ and subband energy fluctuations $\delta E << \Delta E$. Furthermore, the Fermi level E_F should be sufficietly low to avoid population of the excited QWR states. While the above restrictions hold for any attempt to realize reduced dimensionality, there are additional constraints imposed on QWRs acceptable for optoelectronics applications. First, the QWR interfaces should be free of defects in order to minimize nonradiative interface recombination effects which reduce quantum efficiency and carrier lifetime. To achieve this objective, fabrication

techniques which the QWRs are formed completely *in situ* during epitaxial growth is very attractive. Second, in order to ensure adequate interaction between the confined carriers and the photons, high density and uniform arrays of QWRs are desirable. Third, an efficient mechanism of carrier capture from the surrounding barriers into the QWR potential wells is essential to efficiently utilize the excess carriers. From these point of view, triangular-shaped QWRs formed using MOCVD selective growth technique are considered to be very promising for applications to optical devices.

Further improvement in device performance requires increasing the QWR subband separations, particularly in the valence band, in order to minimize thermal population of the higher energy states, and enhancing carrier collection to reduce current leakage effects. Employing strained QWR structures should increase the heavy hole 1D subband splitting due to the lower heavy hole effective mass. Therefore, interest was recently extended to the strained InGaAs/GaAs system. In fact, low threshold current and high modulation frequency have been achieved in quantum well lasers. In addition, recent theoretical studies have shown that the strain effects in QWR structures lead to additional improvements of the lasing characteristics compared with unstrained GaAs/AlGaAs quantum wire lasers.[41-43]. It was pointed out that an introduction of compressively strained QWRs into lasers is very effective for further improvements in their operation characteristics since energy separation between quantized levels in the valence band would be larger due to a smaller effective mass of holes[44]. Thus it is important to obtain such strained QWR structures.

In this chapter, we review the fabrication technique of GaAs and InGaAs quantum wires with the lateral width of about 10-30 nm using the MOCVD selective growth. The optical properties of the QWRs are also discussed using photoluminescence, photoluminescence excitation measurements, and near-field scanning optical microscopy.

2.2 Fabrication Process of Triangular-shaped Quantum Wire Structures

In this section, we briefly review the fabrication technique of GaAs and InGaAs quantum wires developed by Tsukamoto *et al.*[25]. Figure 2.1 shows the fabrication process for the triangular-shaped quantum wires. The selective growth was carried out on masked GaAs substrates with a low pressure (100 Torr) horizontal MOCVD reactor. Source materials for group III elements were trimethylgallium (TMG), trimethylalminium (TMA), and trimethylindium (TMI). Before the growth, SiO_2 line patterns towards [0-11] direction were formed. 200 nm-thick SiO_2 thin films are formed with a magnetron sputtering systems. Photoresist (TSMR CR-B) gratings with a period of 250 nm were defined on the SiO_2 films by a holographic photolithography technique (He-Cd laser: 325 nm). The resist pattern was transcribed to the SiO_2 layers using wet chemical etching with buffered HF. After patterning, the GaAs triangular prisms with (111)A facet sidewalls are selectively grown on the substrates. Further growth leads to the formation of smooth (111)A facet sidewalls, making the dimension of the triangular prism uniform. As a result, a sharp V-groove corner between the triangular prisms is obtained. The space between the triangular prisms is filled up with an $Al_{0.4}Ga_{0.6}As$ layer by switching the growth layer from GaAs to AlGaAs. After the AlGaAs layer was grown, GaAs or InGaAs layer are *in situ* grown between the triangular prisms as quantum wires. The quantum wires are connected to thin quantum wells on (111)A facets. The growth temperature and pressure are 700 ^{o}C and 100 Torr, respectively. V/III

ratio is about 100. The size of the quantum wires can be controlled easily by changing the growth time.

The fabrication of InGaAs quantum wires is the same as that for the GaAs quantum wires because the growth behavior of InGaAs is quite similar to that of GaAs[45]. That is, the growth rate toward (100) direction is much faster than that of (111)A direction.

A schematic illustration and a high resolution backscattered electron image are shown in Fig. 2.2. Even if there is some lateral size fluctuation in SiO_2 mask, the quantum wires are formed uniformly. This is due to the relaxation of the size deviation by the lateral selective growth of the triangular prisms. This is one of the most important features of this fabrication technique.

In addition, a well pronounced vertical layer of Ga-rich AlGaAs is clearly visible at the bottom of the V-groove as shown in Fig. 2.3 (a). This narrow stripe of lower bandgap AlGaAs forms a vertical $Al_xGa_{1-x}As/Al_yGa_{1-y}As$ ($x < y$) QWL (VQWL). The Ga-rich AlGaAs are formed along the grooves as a result of higher migration efficiency of Ga species than that of Al species from the (111)A sidewall plane to the bottom of the V-grooves. The thickness of the VQWL was about 10 nm. Al composition x is considered to be about 0.3 judging from the PL peak position. The VQWL plays an important role in collecting excess carriers and guiding them into the QWRs[46]. We can also see necking where the side QWL connects to the QWR crescent. Similar structures were observed by Gustafsson *et at*[47].

2.3 Optical Properties of GaAs, InGaAs Quantum Wires

2.3.1 Photoluminescence at low temperatures

Optical properties of GaAs quantum wires at low temperatures were investigated by Tsukamoto *et al*[25, 48, 49].Therefore, in this section we concentrate mainly on the optical properties of the InGaAs quantum wires. Figure 2.4 shows the PL spectra of the sample (InGaAs quantum wires) with various lateral dimensions measured at 14 K. The sample was pumped by an Ar^+ laser. In this figure, the hatched spectral region corresponds to PL from the quantum wires. For example, when In composition x is about 0.24, the PL peak at 1.53 eV corresponds to that of the quantum wires. The PL peaks at 1.51 eV and 1.49 eV come from the GaAs bulk transition, probably (D_O, X), and the transition at carbon impurities, respectively. The peak around 1.57 eV originates from the quantum well regions on the (111)A facet sidewalls of the AlGaAs layers. The PL peak around 1.9 eV is from AlGaAs regions. The intensity of PL from the QWRs is comparable or strong compared with other peaks. Similar QWR structures were fabricated on non-planar substrate by several groups[50-53]. In their PL measurements using the QWRs, PL intensity of QWRs are relatively weak because QWLs on non-etched areas serve as traps preventing carriers from reaching QWRs[53]. On the other hand, such QWLs don't exist in our structure and excited carriers are efficiently captured into the QWRs.

As shown in Fig. 2.4, the PL peak positions of the QWRs are systematically shifted to the lower energy side with increasing In

composition. Here, we assume that In composition of these quantum wire structures is the same as that of InGaAs bulk grown under the same conditions. It should be noted, however, that the diffusion larger of In species is longer than that of Ga. Therefore, the In composition in the quantum wires on the patterned substrate is a little higher than that of bulk grown on flat substrates[33]. On the basis of the fact that the growth behavior of InGaAs is quite similar to that of GaAs[45], the lateral width of the quantum wire is estimated to be in the range of 10 to 13 nm. The quantized energy of electrons in the triangular-shaped quantum wires with the lateral width of L_W is almost equal to that in the rectangular-shaped quantum wires with the lateral width of 0.6 L_W[54, 55].

Figure 2.5 (a) shows the PL peak position versus In composition. Theoretical results calculated in terms of a one-band model with and without taking account of the biaxial strain effects are also shown by a dashed line and a solid one, respectively. In the calculation, the biaxial strain effects are the same as those in the quantum wells. When In composition is low, the photon energy is almost on the dashed line. With the increase of In composition, however, it deviates from the dashed line and approaches the solid one. This suggests that the strain is relaxed with the increase of In composition owing to the approach of the structural dimensions to the critical thickness conditions.

Figure 2.5 (b) is the relationship between In composition of the quantum wires and the FWHM of the PL spectral line. As shown in this figure, the FWHM suddenly increases at x = 0.4. Consequently, on the basis of both the FWHM and the peak position of the PL we can conclude that the dimensions of the quantum wires exceed the critical

thickness at around x=0.3-0.4. Almost the same value of x, on the other hand, gives the critical thickness condition for the quantum wells with the thickness of 5 nm. These results suggest that the strain effects of our quantum wires can be modeled in the same way by the biaxial strain effects as that for conventional strained quantum wells, which is consistent with the fact that the present quantum wires are connected to the quantum well regions. The change of FWHM with the increase of In composition is more marked than that of PL peak positions. For reference, we also measured FWHM's of InGaAs (5 nm) / GaAs quantum wells with various In compositions and obtained similar results. Therefore, these results suggest that the influence of strain relaxation, in general, is mare markedly exhibited by the change of FWHM of PL peaks than that of the peak positions. With respect to a critical thickness for the triangular shaped strained QWRs, theoretical analysis was performed by Freund *et al*[56].

In addition, the broadening of FWHM with increasing In composition may be due to the exciton localization effects at In-rich zones because of the segregation effects[57].

Figure ? displays PL spectra of the sample with and without (InGaAs) QWRs. The peaks at around 1.94 eV and 1.87 eV are attributed to $Al_{0.4}Ga_{0.6}As$ bulk and VQWL, respectively. Al content of VQWL can changes by changing growth conditions[58]. It should be interesting to realize gain coupled DFB lasers with VQWL s as active material.

2.3.2 Temperature dependence of photoluminescence

Figure 2.6 shows the dependence of PL spectra of GaAs QWRs on temperature. The excitation power was 3 mW (an Ar^+ laser). As shown in this figure, clear emission peaks of the QWRs are observed up to room temperature. The peaks of side wall quantum wells decrease rapidly with increasing temperature due to the carrier thermalization into QWR and disappears at about 180 K beyond which only the QWR emission peak remained. The QWR peak could be observed easily even at room temperature. A weak shoulder at the shorter wavelength side begins to emerge at higher temperature. This is attributed to emission between higher order subbands.

PL peak energies are plotted as a function of temperature in Fig. 2.7. The peaks of 50 nm thick GaAs QWL and calculated peak of GaAs band gap are also given in the figure. All the peaks showed the similar tendency to the GaAs band gap. The temperature dependence of the luminescence spectra does not show any blue shift of the emission line, which is usually ascribed to the thermal activation of localized excitons. In the case of $In_{0.2}Ga_{0.8}As$ QWRs, however, the value of energy shift was rather small up to 100 K.

Although the reason is not unclear, we can interpret the result as follows. A blue shift due to the thermalization effect of excitons can be larger than in other QWRs, resulting in smaller red shift of emission line. InGaAs QWRs with higher In content have larger FWHM as discussed in Section 2.3.1. This means alloy disorder is larger in InGaAs QWRs. Therefore, thermalization effect of excitons can appear

more remarkably in InGaAs QWRs than in GaAs QWRs or InGaAs QWRs with smaller In content.

The full width at half-maximum (FWHM) of the lowest lying electron-heavy hole (1e-1hh) peak was calculated from the PL peaks in Fig. 2.8 (a). For higher temperature spectra, the 1e-1hh peaks were separated from the higher subband peaks by assuming two Gaussian distribution functions. As a reference, FWHM values of QWL sample are also displayed in the figure. In the case of the QWL, the FWHM increases with increasing temperature almost linearly up to room temperature. This is consistent with the theoretical prediction of the 1e-1hh subband to subband transition of QWR structure in which the density of states is step like.[59]. On the other hand, the FWHM of QWR showed very different features from QWL. The FWHM firstly increases linearly with increasing temperatures. However, the broadening of the FWHM was suppressed at high temperatures especially in InGaAs QWRs. There results can be attributed to the distributed density of state in QWRs. Similar tendency was observed by Wang *et al*[52].

At the present stage, however, we could not fully understand the linear temperature dependence at low temperatures of the QWR FWHM. The linear dependence of QWR FWHM at low temperatures may be due to some potential fluctuations resulting from the small wire size fluctuation. Photogeneraged excitons are localized at the potential minima at low temperatures and thermalized into higher energy levels as temperature is increased.

Figure 2.8 (b) shows the dependence of integrated PL intensities on temperature. The PL intensities are normalized with intensities at

12 K. The PL intensity of QWRs decreased by the order of 2 (approximately 1/50 of the intensities at 15K). This characteristics are better than that of GaAs quantum wells. This indicates that the confinement of carriers in the QWRs is sufficient and the QWRs fabricated by this technique are very promising for applications to optical devices in room temperature operation.

2.3.3 Photoluminescence excitation measurements

Photoluminescence excitation (PLE) measurements of triangular -shaped QWRs were previously performed by S. Tsukamoto *et al.* [25] They observed clear distinct polarization anisotropy associated with QWRs. We investigated the more detailed PLE characteristics of the QWRs at low temperatures (12-150 K) using a tunable Titanium:Sapphire laser. GaAs and InGaAs QWRs (L_X=30 nm) was used in these experiments. The polarization of the laser beam was changed by using a polarizer and a half-wave plate.

The detected photon energies were fixed at higher energy sides of PL peaks. The excitation power was 1-5 mW. Figure 2.9 displays the PLE spectra of GaAs and $In_{0.06}Ga_{0.94}As$ quantum wires measured at 12 K. In the spectrum of GaAs QWR, calculated levels are also shown. The levels were calculated in the effective mass approximation using a finite well model with $\Delta Ec/\Delta E_g=0.6$[60]. These spectra show well resolved peaks (up to 3rd excitation levels) due to absorption at their 1D subbands. The spectra measured with an exciting beam polarized parallel or perpendicular to the QWRs show distinct polarization anisotropy associated with valence band mixing. The Stokes shift between PL and PLE amounts to 30 meV. These Stokes shifts arise from potential fluctuations along the QWR direction, caused by size fluctuations and Al contents variations in surrounding barriers, and by the microscopic disorder of In inherent to the ternary alloy systems. Higher subband show a larger joint density of states, as is expected from the crescent shape of the wires[51]. In Fig. 2.10, we compare PLE spectra taken with the detection energy

set on several points of the PL profile of the QWR. The peaks appearing in the PLE spectra are more pronounced when the detection energy is on the high-energy side of the PL peak. This is considered to be due to the inhomogenities of the QWRs. In order to obtain better definition, the detection energies were set on the higher energy side of the PL peaks in our experiments. The spectral positions of the peaks don't show little shifts.

Figure 2.11 shows the PLE peaks plotted as a function of temperature for GaAs and $In_{0.06}Ga_{0.94}As$ QWRs. As shown in the figure, the peaks shift to lower energies, reflecting the band gap shrinkage. The Stokes shift is expected to vanish at higher temperatures comparable to the potential fluctuations[57]. In our experiments, however, the Stokes shift did not change up to 150 K in both case of GaAs and InGaAs QWRs. In addition, some strange features manifests itself in the higher subbands in both cases. Subband separation between adjacent PLE peaks of the GaAs QWRs is more than 50 meV, which corresponds to 2 k_BT_{room}. This value is larger than the similar shaped QWRs (45 meV)[61]. This result indicates that our QWRs have narrower lateral potential profiles. Further optimization of the structures and the growth conditions (Al content, temperature, etc.) will increase the subband separation up to 3 k_BT_{room}. In addition, subband separation of InGaAs QWRs is larger (about 70 meV) than that of GaAs QWR. This is probably due to deeper potential profiles caused by InGaAs. The separation between the 1st electron-heavy hole (hh) and electron-light hole (lh) transitions in the case of InGaAs QWRs is larger than in the case of GaAs QWRs (38 meV, 25 meV, respectively). This is attributed to compressive strain effects in

the quantum wires, which generally enhance the separation between hh and lh. For device operation at room temperature, subband separation is very important in order to minimize thermal population in the higher energy states, and carrier collection into the QWRs.

2.3.4 Photoluminescence observation with near-field scanning optical microscopy

The QWRs have some structural fluctuation as discussed in the previous sections and their inherent properties (for example, sharp luminescence peak) are screened. Therefore, it is important to observe optical properties of local areas of the QWRs. Local excitation is expected to make the PL spectral width narrower. The invention of the aluminum coated, tapered fiber probe, and the subsequent developments in near-field scanning microscopy (NSOM)[62] have enabled us to build a near-field scanning optical microscope for use in spectroscopic studies. In relation to QWRs, low temperature NSOM measurements were demonstrated with the T-shaped QWR array. In 1996, the near-field spectroscopic characteristics of nanostructures (QDs) were studied[63] with the NSOM.

In this section, we discuss the observation of spatially resolved photoluminescence spectra from GaAs triangular shaped QWRs, using a near-field scanning optical microscope (NSOM)[64].

Figure 2.12 shows the experimental setup and the structure of the sample. The cap layer and upper AlGaAs barrier layer were thinned to 70 nm so that sub near-field luminescence can be detect. The sample was excited by an Ar^+ laser through a tapered fiber tip. This is called "illumination mode". The aperture size is about 100 nm. The fiber tip was coated with aluminum to obtain large optical confinement. PL was collected by a lens and detected by single monochromator and optical multichannel analyzer. In order to control the tip-sample separation, a shear-force technique was employed.

The shear-force image and near-field PL spectra at room temperature were shown in Fig. 2.13. The excitation power was 1-10 nW. In the case of near-field measurements, the tip was kept about 10 nm from the surface of the sample. The PL peak around 1.53 eV and 1.62 eV originate from the QWR and the QWL on (111) A, respectively. A single QWR is thought to be excited because the excited area was about 200 x 200 nm. As can be seen in the figure, we can observe some sharp lines. These peaks were reproducible and it was confirmed that they were not laser lines. Therefore, we can conclude that they are from the QWR. This result designate that there is fluctuation not only between the QWRs but along each QWR. From AFM observation, it was ascertained that there were fluctuations composed of atomic steps at the corners of the V grooves along the QWR. The period of the steps depends on the angle of the misalignment of line patterning (typically, 20 nm). Therefore, we can see several sharp lines. We believe that every sharp line was from the single QWR. It is difficult to distinguish signals from noise at this stage because the PL is rather weak due to the room temperature measurements. It should be noted that the excitation area may be wider than expected due to carrier diffusion, as the cap and barrier layers are a little thick for near-field excitation.

2.3.5 Cathodoluminescence measurements

Cathodoluminescence (CL) microscopy is one of the most useful characterization techniques for two dimensional visualization of interface structures. In order to identify the origins of the PL peaks, we performed CL measurements at low temperature (10-20 K). The luminescence generated by a 3 kV electron beam with 0.2 nA current was collected by a mirror and its spectrum was analyzed as a function of position (x, y) over the epitaxial layer. The magnetic field of 0.2 T was applied to suppress the carrier diffusion and improve spatial resolution. Figure 2.14 shows a CL spectrum and spectrally resolved intensity images recorded at the three photon energies marked in the spectrum. The resolution in wavelength was 2.5 nm. SEM images are also shown. The CL spectrum was recorded over an area of 2 x 2 μm^2. Figure 2.14 (a) clearly shows line-shaped emissions from the bottoms of the V grooves, where the QWRs are expected to be located. Though there is distribution of the emissions, they are not random; some 1 μm-long line-shaped emissions can be observed. These line-shaped emissions probably originate from misalignment of photolithography. The peak B originates from the thin QWL at the (111) A side-walls of the V grooves. The emissions are no longer line-shaped. Figure 2.14 (c) indicates that peak C also comes from the bottoms of the V-grooves. The emissions probably come from the VQWLs. Though the emissions are also line-shaped, their lengths are longer than that from the QWRs. The effect of the misalignment was reduced due to two dimensionality.

Figures 2.15 and 2.16 show the spatial CL images measured at intervals of 10 nm, from 660 nm to 730 nm and 770 nm to 790 nm, respectively. At around 700 nm (sidewall QWL), PL emitting positions depend on the detecting wavelength. Therefore, we conclude that the broadening of the PL peak is due to the size fluctuation between the QWLs. In the case of the QWR (around 780 nm), we can draw the same conclusion.

2.4 Concluding Remarks

In Chapter 2, the fabrication technique of GaAs and InGaAs quantum wires using the selective MOCVD was reviewed. The optical properties of the QWRs are also discussed by using photoluminescence (PL) measurements, photoluminescence excitation (PLE) measurements, measurements with near-field scanning optical microscope (NSOM), and cathodoluminescence measurements (CL). Temperature dependence of the FWHMs demonstrated that the broadening of emission peak of the QWRs are suppressed at higher temperature, which probably reflects the density of states in QWRs. From the temperature dependence of PL intensity, the QWR structures are promising for applications to optical devices such as laser diodes and optical switching devices operated in room temperature. PLE results exhibited clear peaks corresponding to the quantized transition levels and the anisotropic polarization dependence. The subband spacings for the GaAs QWRs was rather large (50 meV) and the spacing was enhanced by introducing strained InGaAs QWRs. NSOM measurements at room temperature demonstrated the sharp lines from the QWRs. The origins of the PL peaks were identified with CL measurements.

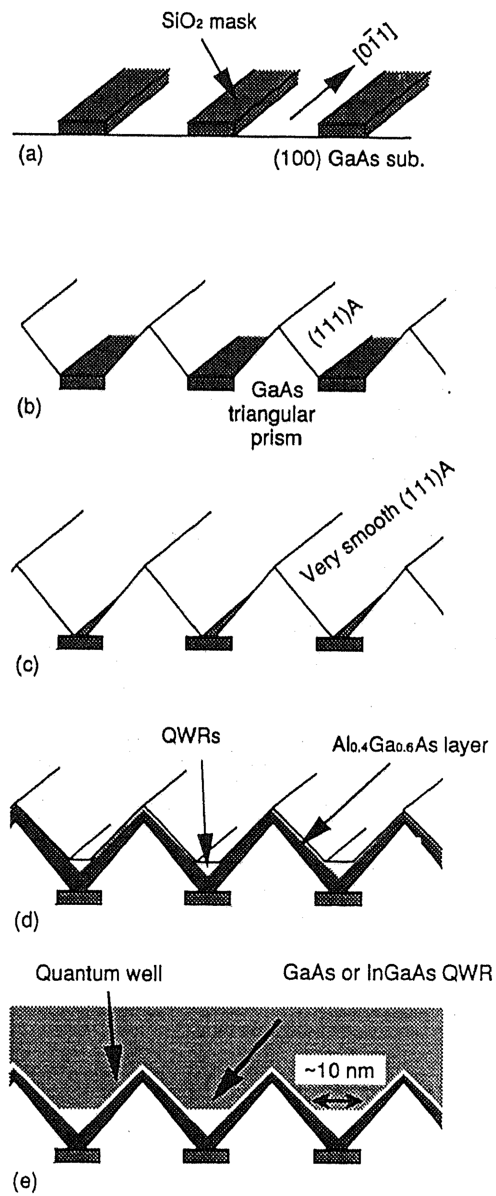

Fig. 2.1 Fabrication process for the triangular-shaped quantum wires using the selective MOCVD growth.

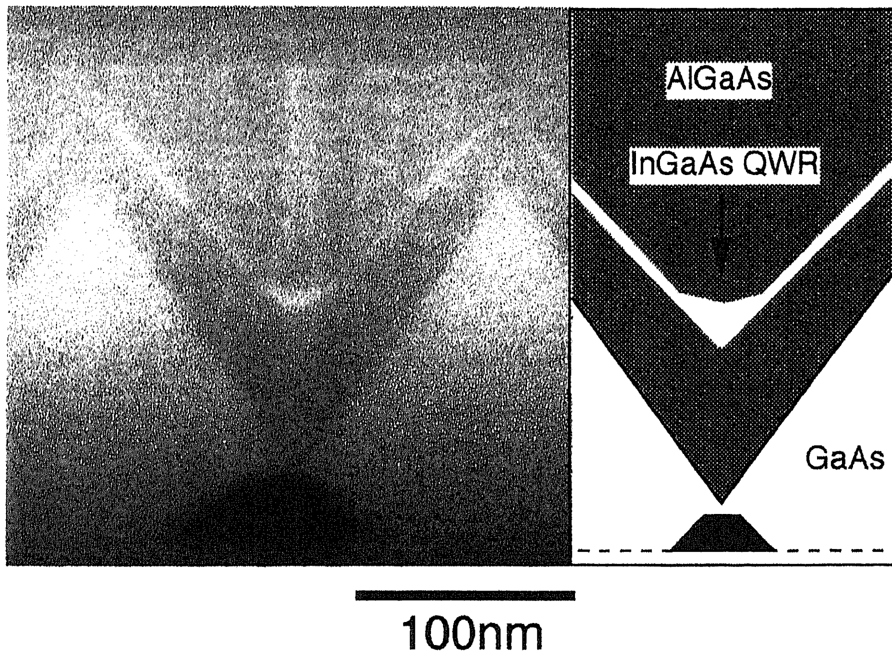

Fig. 2.2 A high-resolution backscattered electron image and a schematic illustratinon of the triangular-shaped $In_{0.1}Ga_{0.9}As$ quantum wire.

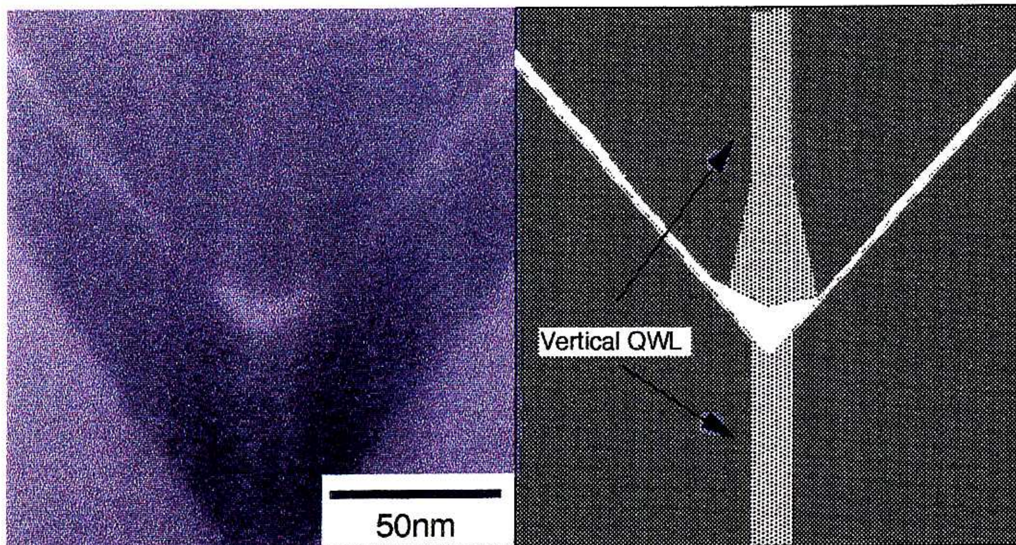

(a)

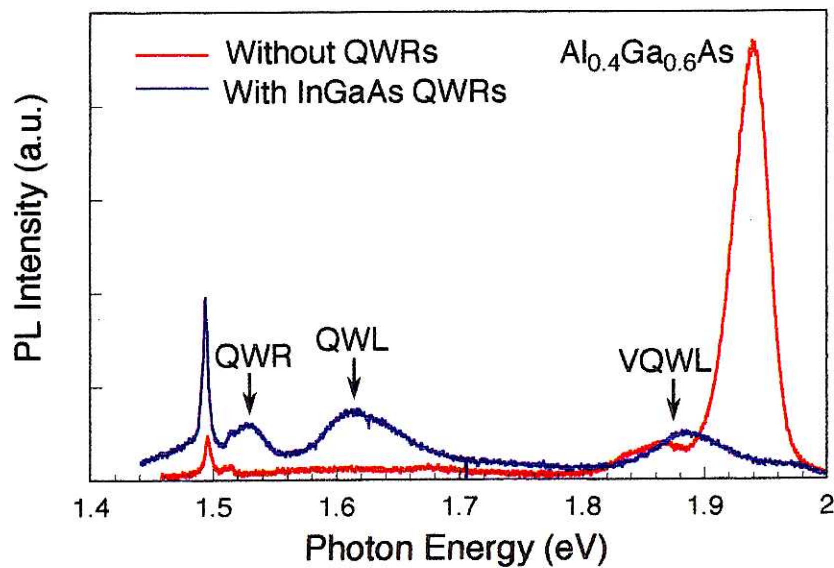

(b)

Fig.2.3 (a) A high-resolusion backscatterd electron image of the InGaAs quantum wire. Vertical Ga-rich region (vertical quantum well) can be observed. (b) PL spectra of the samples with and without $In_{0.12}Ga_{0.88}As$ QWRs.

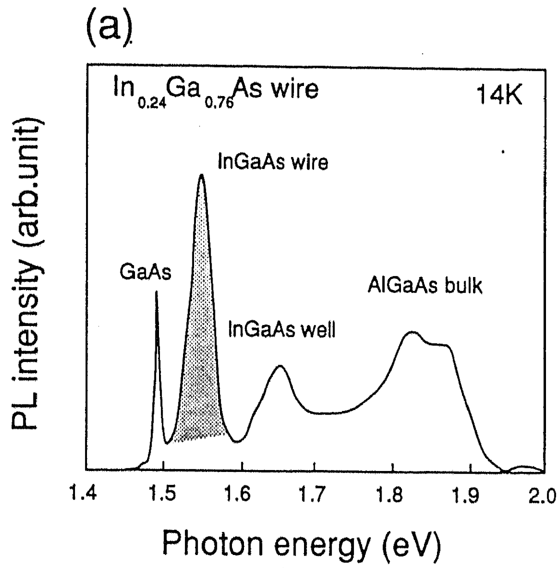

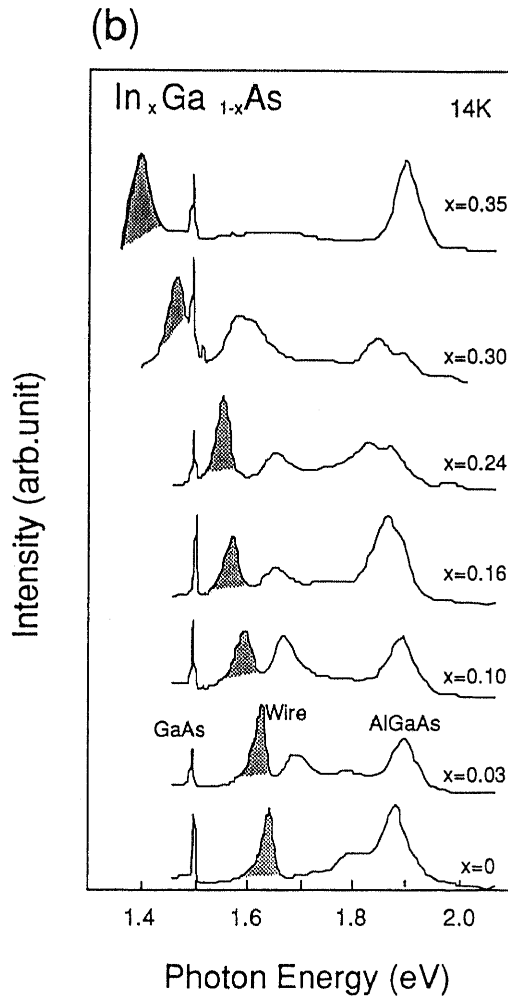

Fig. 2.4 PL spectra of the InGaAs quantum wires with various Indium compositions at 14 K (hatched spectral region corresponds to PL from the quantum wires).

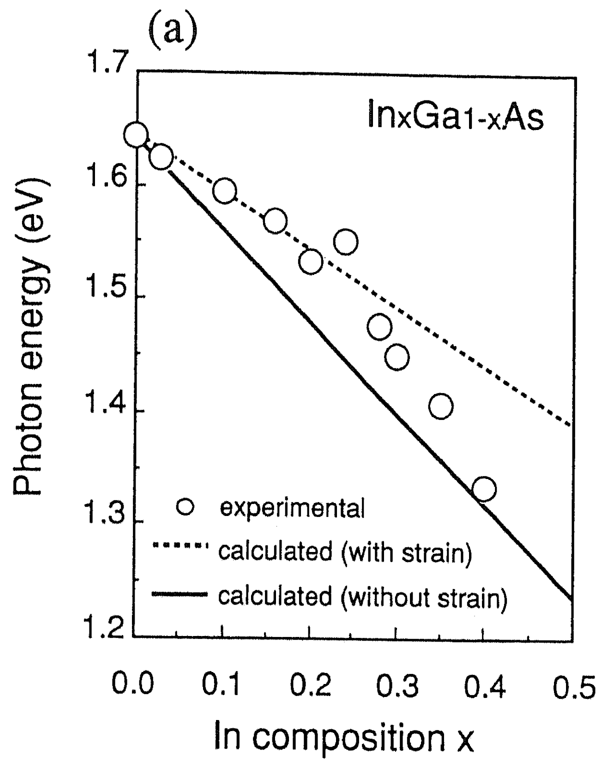

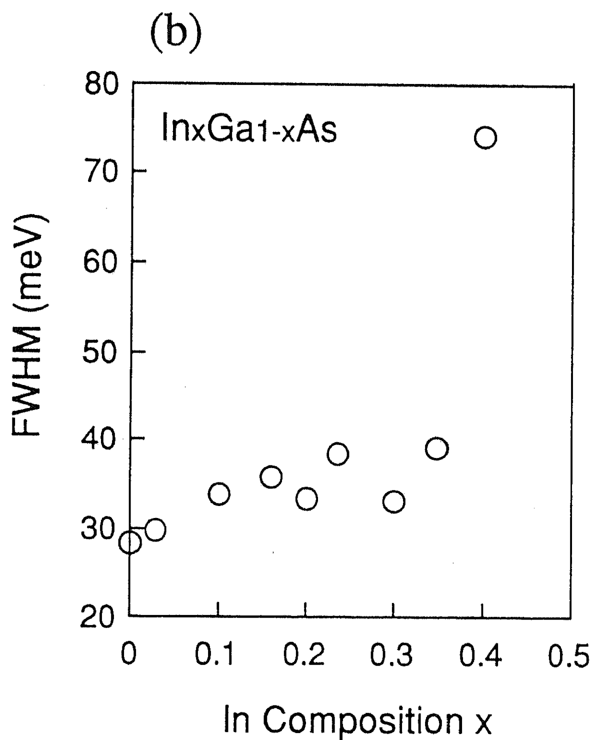

Fig. 2.5 (a) PL peak position plotted as a function of In composition x. (b) Relationship between In composition of the quantum wires and the FWHM of the PL spectral line.

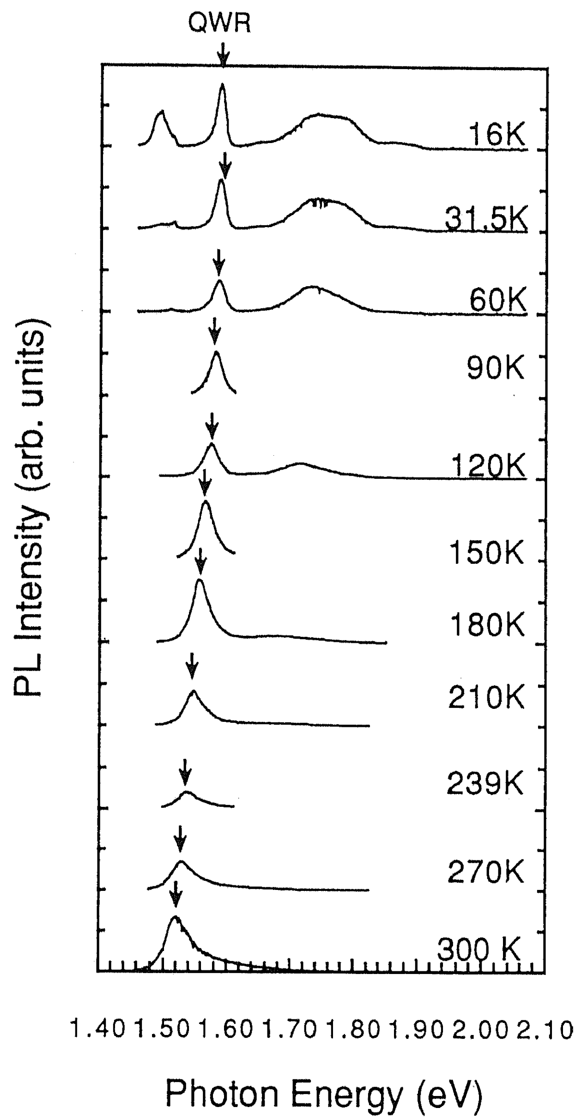

Fig. 2.6 Dependence of PL spectra of the GaAs quantum wires on temperature.

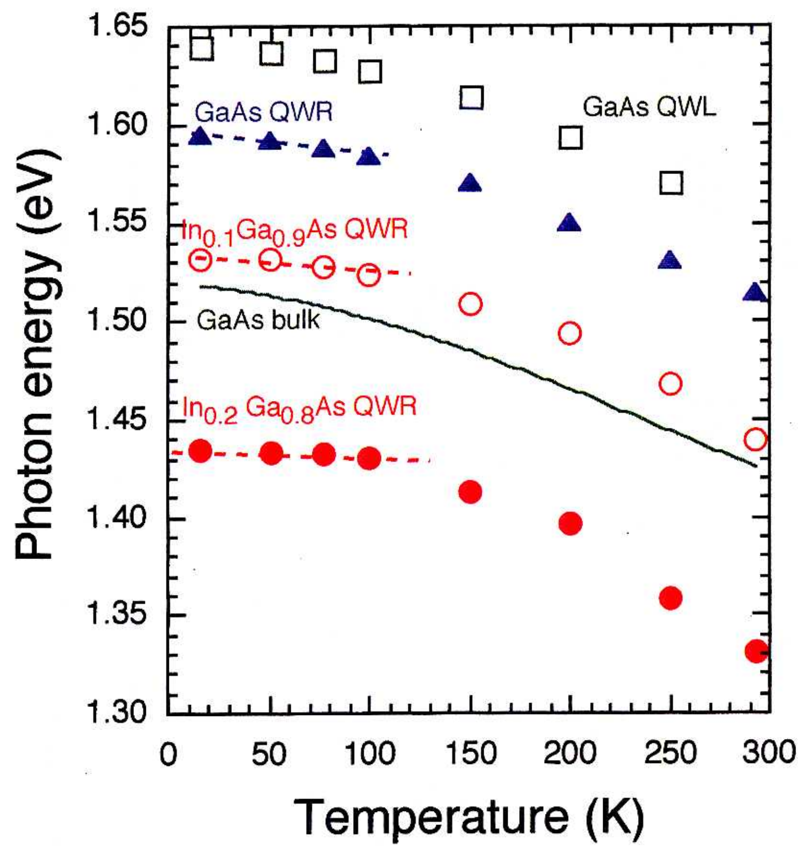

Fig. 2.7 PL peak energies of QWRs as a function of temperature.

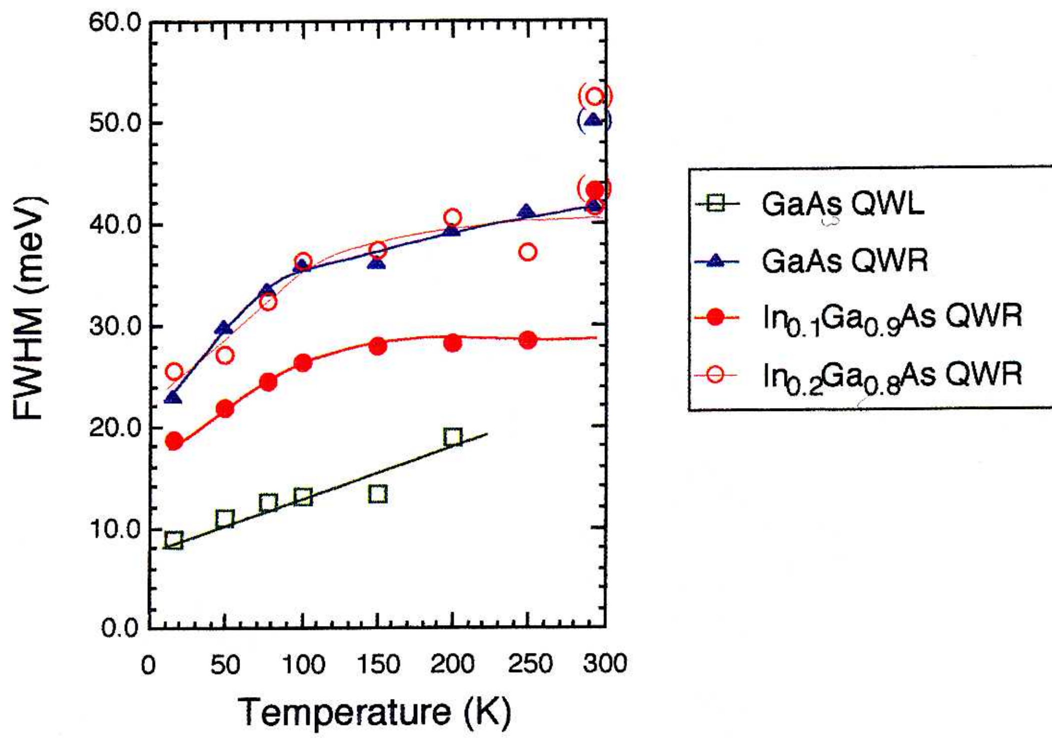

(a)

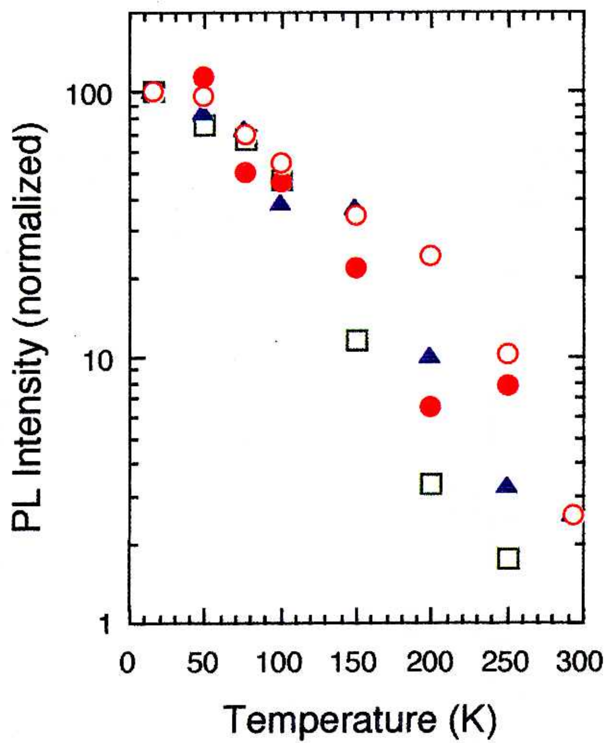

(b)

Fig. 2.8 Dependence of PL from GaAs and InGaAs QWRs on temperature. (a) FWHM of PL peaks , (b) PL intensity.

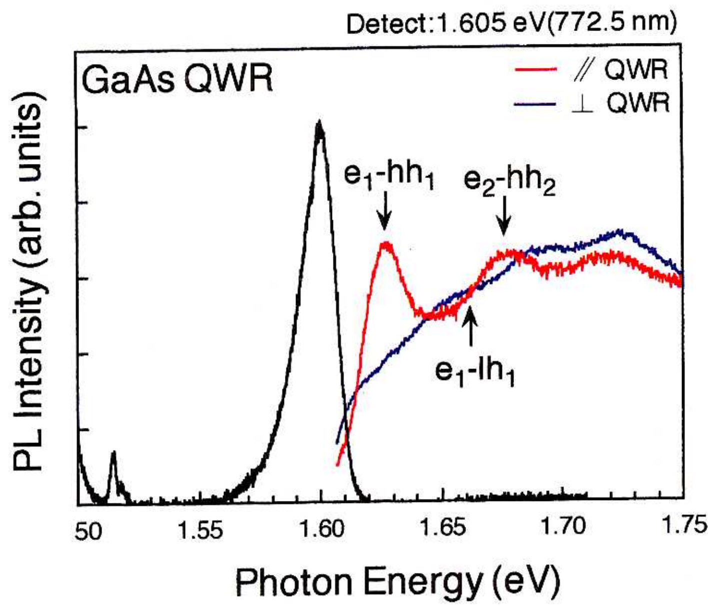

(a)

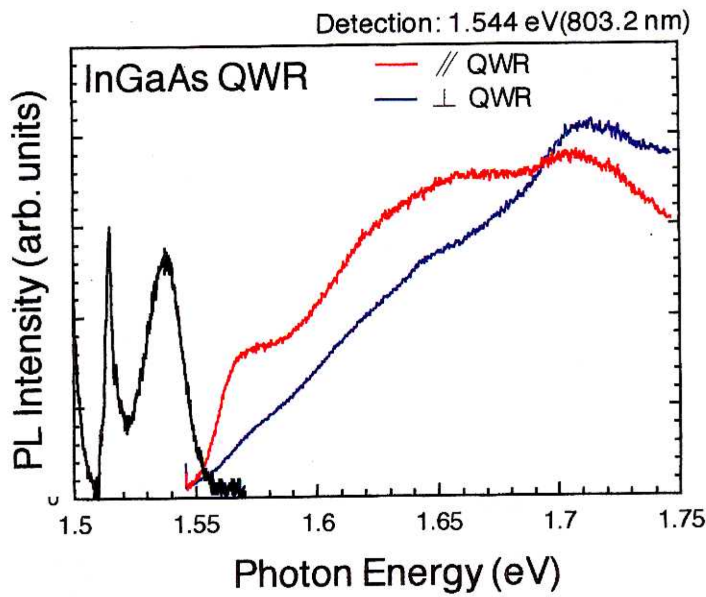

(b)

Fig. 2.9 Low temperature (12 K) polarization dependent PLE and PL spectra for (a) GaAs QWRs, (b) $In_{0.06}Ga_{0.94}As$ QWRs.

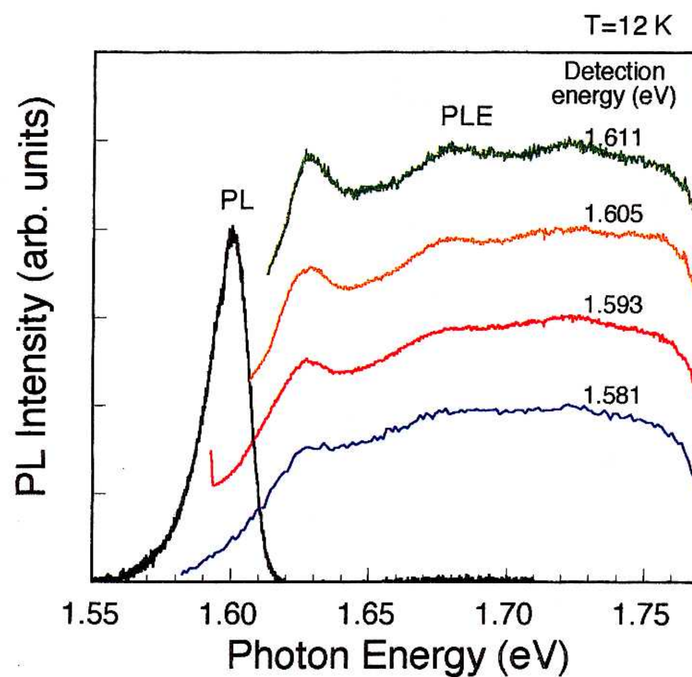

Fig. 2.10 PL spectrum and PLE spectra of the GaAs QWRs/ Polarization of the exciting laser is set parallel to the QWR axis.

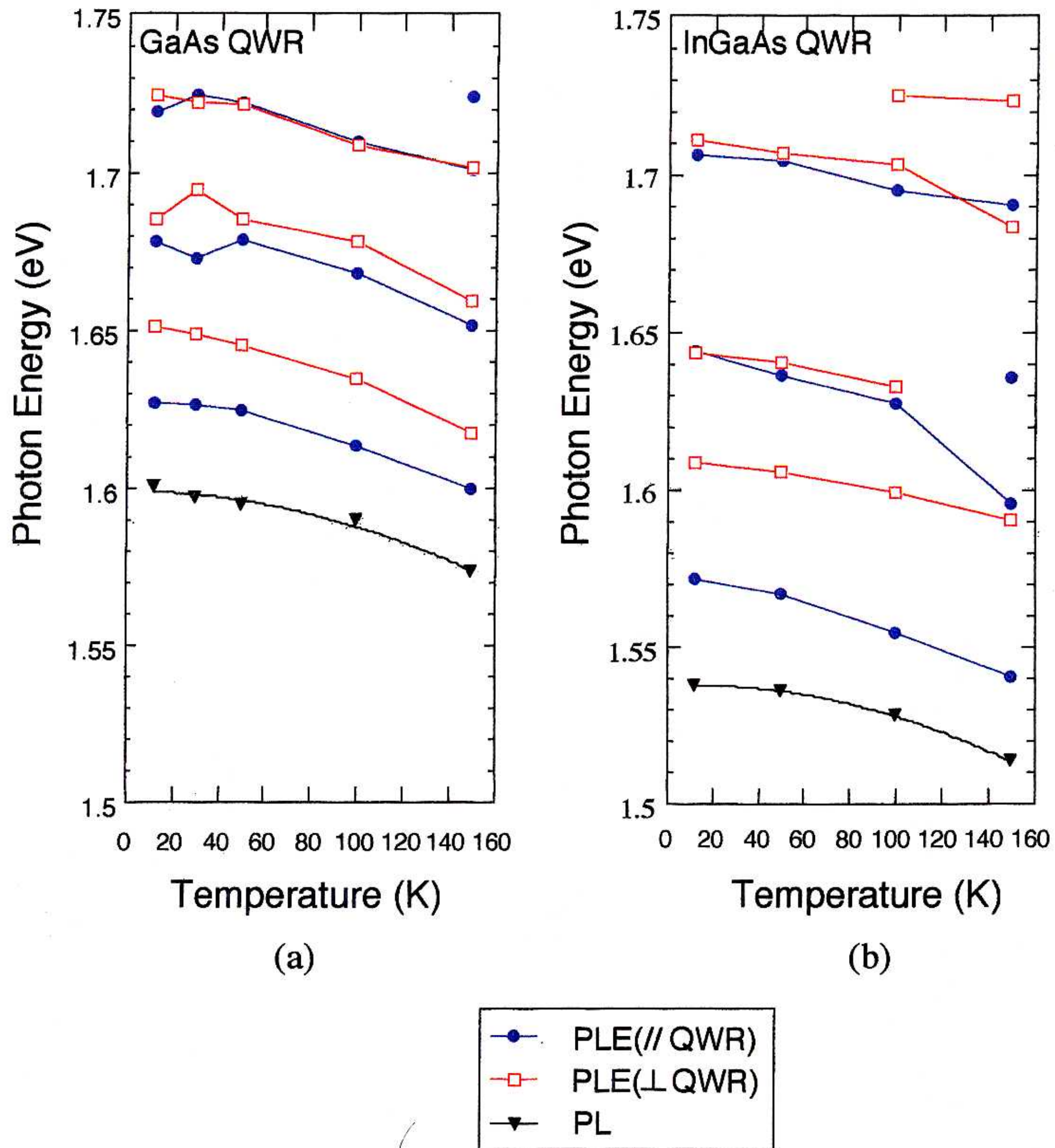

Fig. 2.11 PLE peaks plotted as a function of temperature for (a) GaAs QWR, (b)InGaAs (In:0.06) QWR

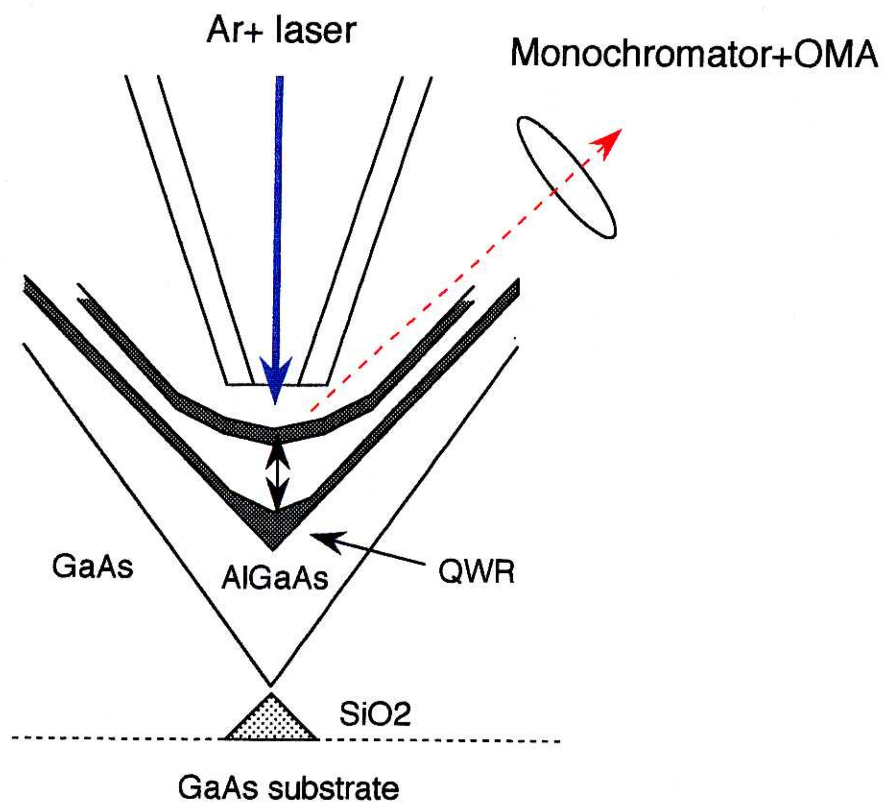

Fig. 2.12 The experimental setup and the structure of the QWR sample. The cap layer and upper AlGaAs barrier layer were about 70 nm. The lateral dimension of the QWR was 20 nm and the period was 260 nm.

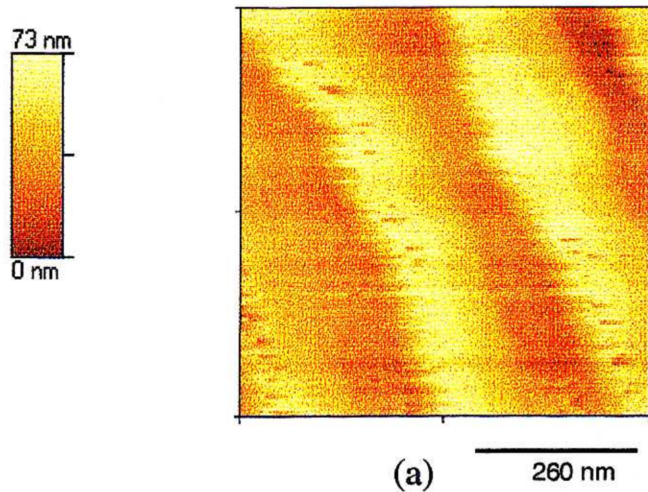

(a)

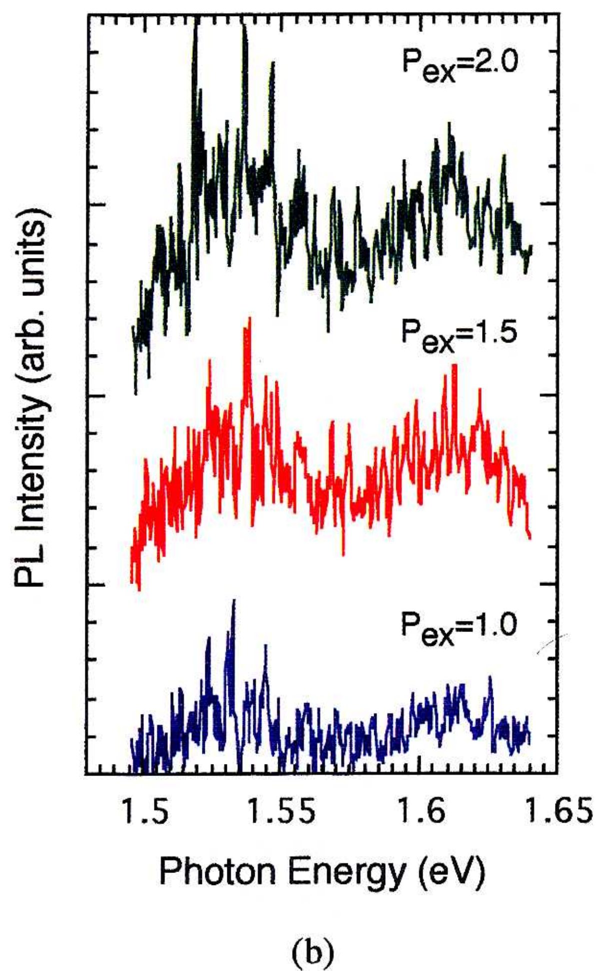

(b)

Fig. 2.13 (a) Shear-force image of the QWR sample. (b)Near-field PL spectra at room temperature with various excitation power P_{ex} (normalized).

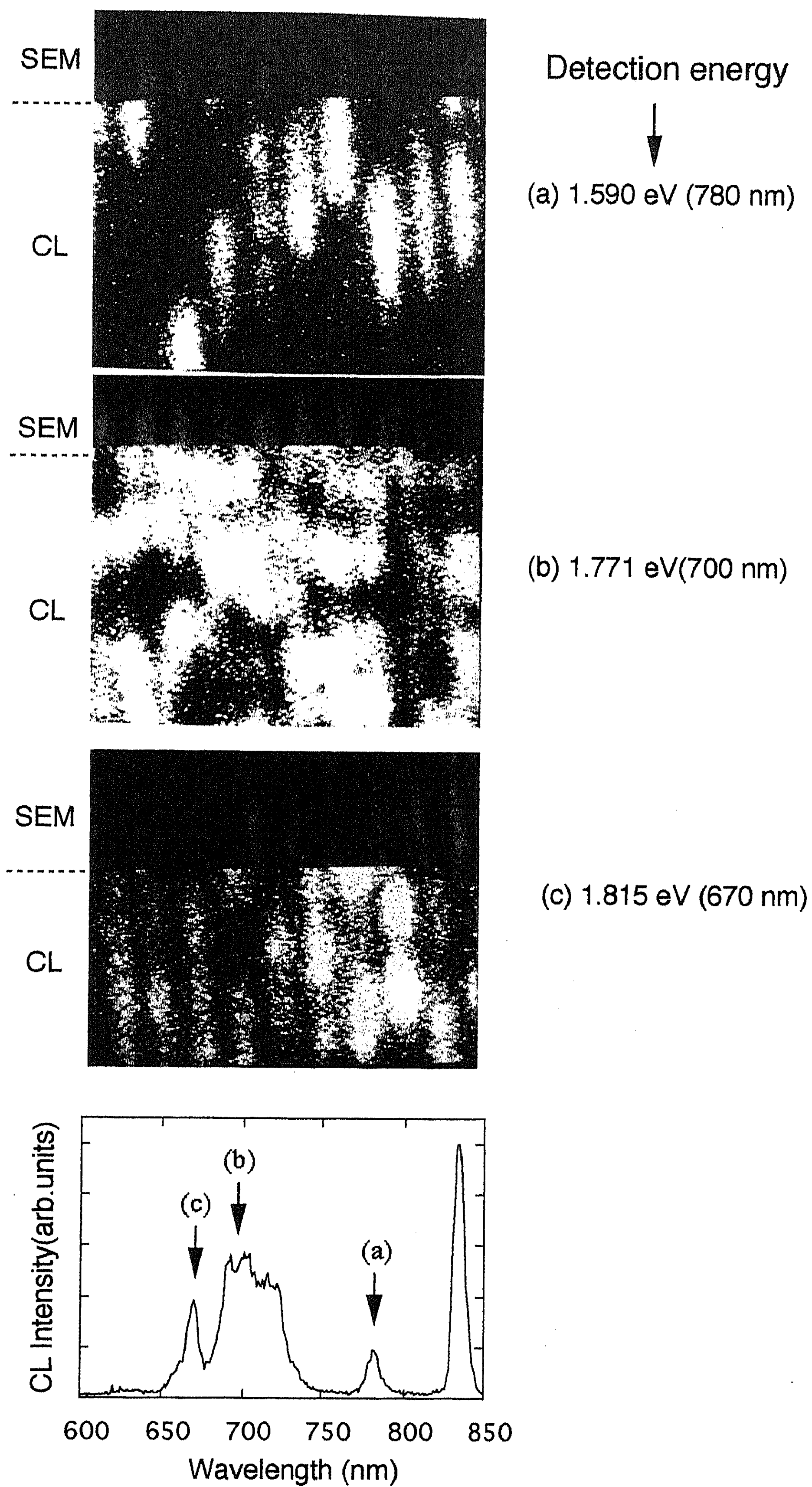

Fig. 2.14 A cathodoluminescence spectrum and spatially resolved intensity images at the three photon energies marked in the spectrum.

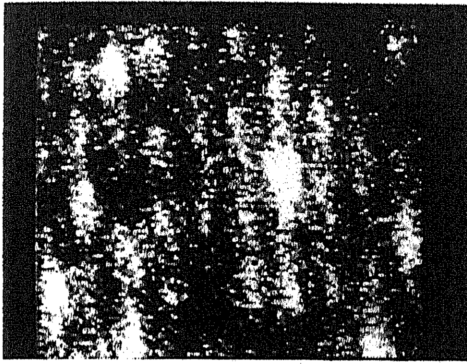

λ=660nm

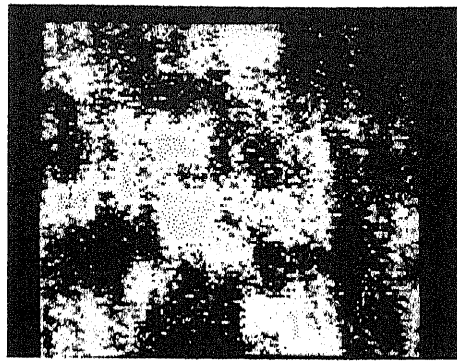

700nm

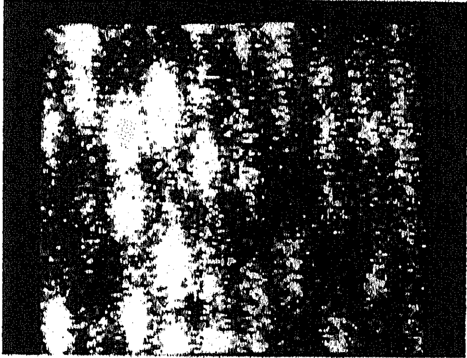

670nm

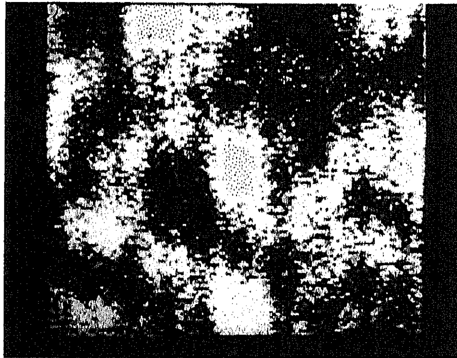

710nm

680nm

720nm

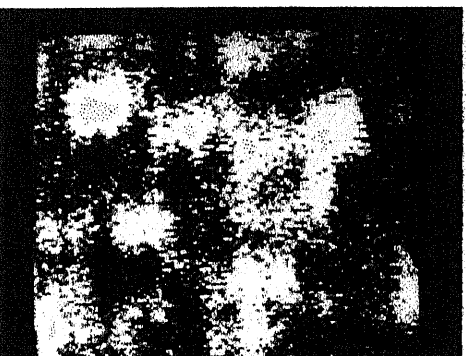

690nm

730nm

Fig. 2.15 Spatial CL images(128x128) measured from 660 nm to 730 nm at intervals of 10 nm.

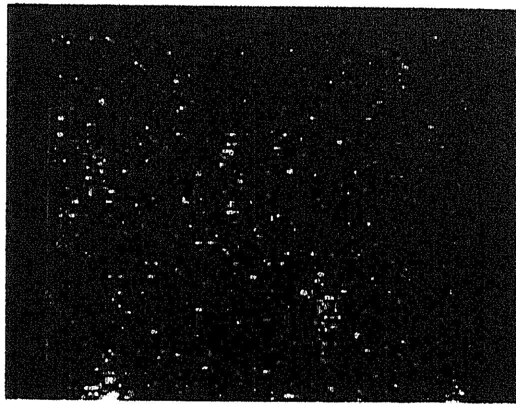

770nm

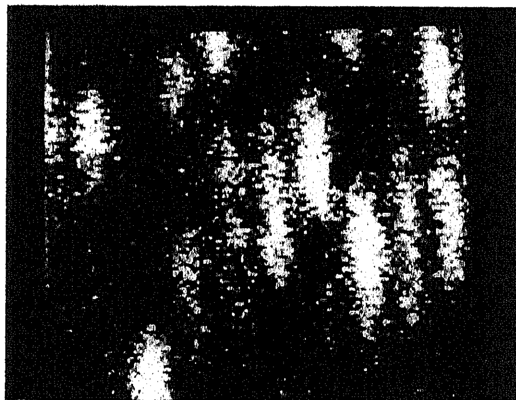

780nm

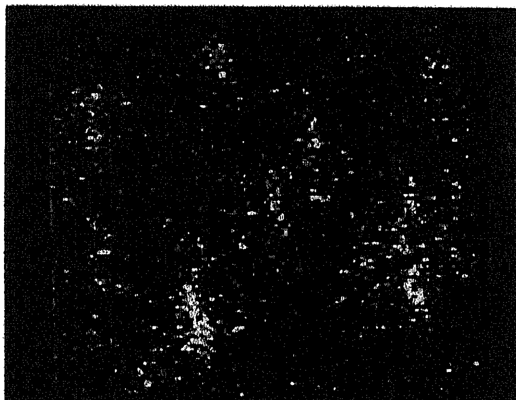

790nm

Fig. 2.16 Spatial CL images(128x128) measured from 770 nm to 790 nm at intervals of 10 nm.

Chapter 3

Fabrication and Optical Properties of InGaAs Quantum Wires Grown on a (110) Cleaved Plane of AlGaAs/GaAs Superlattice

3.1 Introduction

As reviewed in Chapter 1, various type of quantum wire (QWR) structures have been fabricated. In order to apply these QWRs to optical devices, sufficient density and volume of QWRs is required, in addition to realization of high quality QWRs. In most cases, electron beam lithography or holographic lithography is used for patterning masks. In these technique, the density of quantum wires is limited by lithographic process and a measure of size fluctuation of mask pattern can not be avoided at this stage. To overcome this problem, T-shaped edge quantum wires have proposed and fabricated[27-29]. However, the lateral carrier confinement of this structure is not sufficiently strong.

On the other hand, there have been several reports on MOCVD and metalorganic molecular beam epitaxy (MOMBE) selective growth using a native oxide layer on semiconductors[65, 66]. There have been several reports concerning MOCVD[65]and metalorganic molecular beam exitaxy (MOMBE)[66] selective growth using a native oxide layer on semiconductors. In MOCVD, the selected are is strongly oxidized to form a very thick (a few micron) oxide layer. In the MOMBE case, a very thin oxidized GaAs surface is used as a

selective mask. These results suggest that a native oxide on semiconductor can function as a selective mask. In both cases, the specific area is selectively oxidized by lithography techniques. However, it might be possible that only an oxide on an AlGaAs layer acts as a selective mask and that an oxide on GaAs does not because AlGaAs is more susceptible to oxidation than GaAs. Therefore, the cleaved facet of AlGaAs/GaAs superlattice has the potential to act as a selective mask pattern. If the cleaved facet of AlGaAs/GaAs superlattice is used as a selective growth mask, quantum wires with high density and very small fluctuation could be achieved. Notomi et al. used this selective growth technique for fabricating quantum wire structures[30]. They fabricated GaAs quantum wires on a V-grooved structure by growing the AlGaAs/GaAs heterostructure on a cleaved facet of AlGaAs/GaAs superlattice. Nevertheless, fabrication of InGaAs quantum wires by the selective growth on a (110) cleaved plane and their optical measurement has not been reported so far.

In Chapter 3, we report the fabrication of ridge-type InGaAs quantum wire structures (lateral width is about 25 nm) using the selective growth on a (110) cleaved plane of AlGaAs/GaAs superlattice. Spatially resolved photo-luminescence (PL) was observed by using a micro-PL (μ-PL) measurement.

3.2 Fabrication of the Quantum Wire Structure

3.2.1 Fabrication process

The fabrication process of the InGaAs quantum wire structure is illustrated in Fig.3.1. First, $Al_xGa_{1-x}As$ (50 nm)/GaAs (12 nm) superlattice was grown. All the samples were grown by low pressure MOCVD and the source materials were the same as that shown in Section 2. Al composition x is 0.6. When Al composition is less than 0.3, the selectivity is weak and polycrystal is deposited on the AlGaAs layer. In particular, when x is less than 0.1, the AlGaAs does not perform as a selective mask at all. The details of native oxide on AlGaAs with various Al contents are discussed in Section 3.2.2. The sample was cleaved in the air and oxidized by a plasma ozone asher (300°C, 5 minutes) to promote the oxidization of AlGaAs layers. Next, GaAs layer was grown on the cleaved (110) facet, and GaAs trapezoids with (111)A and B, (110) facets were formed. In this connection, the growth behavior of GaAs is discussed in another paper [30]. The native oxide on the AlGaAs layer acted as a selective mask and no polycrystal was deposited. InGaAs was grown on top of the GaAs trapezoids as quantum wires. Finally, the quantum wires were buried with GaAs. Before the growth of the first GaAs layer, thermal etching was performed under the condition of 750 ^{o}C for 5 minutes to remove thin oxide layer on GaAs region of the superlattice.

3.2.2 Native oxide layer on $Al_xGa_{1-x}As$

The reactivity of Al with oxygen is larger than that of Ga. Therefore it is expected that the higher Al composition x is, the more susceptible to oxidation AlGaAs becomes. However, higher Al composition is not desirable for optical properties because non-radiative centers will increase. The surface of oxidized layer on AlGaAs mainly consists of Ga_2O_3 and Al_2O_3. While Ga_2O_3 easily desorbs at the growth temperatures, Al_2O_3 is very stable up to high temperatures. It is possible to preferentially oxidize AlGaAs over GaAs[67, 68]. In order to optimize the Al content for formation of oxide layers as a selective mask, we investigated selectivity of oxidized AlGaAs with various Al contents.

The samples which consists of $Al_xGa_{1-x}As$/GaAs superlattices were prepared. Al mole fraction x was changed from 0.05 to 0.4. After cleaving the samples in the air, they were oxidized by a plasma ozone asher (300 ^oC, 5 minutes) to promote the oxidization of AlGaAs layers. $In_{0.1}Ga_{0.9}As$ was grown by MOCVD. The growth temperature was 600 ^oC and the V/III ratio was 20. Before the growth, thermal etching was performed under the condition of 750 ^oC for 5 minutes as shown in Section 2.3.1 to remove thin oxide layer on GaAs region of the superlattice. Scanning electron microscope images and schematic illustrations of the grown surfaces are shown in Fig. 3.2. In the case of x=0.4, InGaAs layer was selectively grown on GaAs layer with good uniformity. AlGaAs native oxide acted successfully as a selective mask.

Below x=0.3, the selectivity became weaker and polycrystals were deposited on the AlGaAs regions. In particular, AlGaAs did not act as a mask at all in the case of x=0.05. Therefore, Al composition should be over 0.4 at least to utilize AlGaAs layer as a selective mask in the above growth condition. In our experiments, AlGaAs was oxidized in plasma ozone atmosphere. The growth characteristics on the samples that were intentionally oxidized in several ways and it was demonstrated that the characteristics were independent of the oxidation process[30]. Concerning the thickness of oxidized layers on AlGaAs, it was reported that the thickness is on the order of 10 Å[30].

3.2.3 Growth behavior of InGaAs on a (110) plane

In order to form the quantum wires on top of the GaAs trapezoids, the growth rate of InGaAs toward (110) must be faster than that toward (111)A or B. Therefore, we examined the growth behavior of InGaAs on the sample to optimize the growth condition. Figure 3.3 shows the growth rate dependence of InGaAs layer on the V/III ratio, Indium composition. In Fig. 3.3 (a), In mole fraction is 0.3. The growth pressure and temperature is fixed at 76 Torr and 600 ^{o}C, respectively. The vertical axis Vertical/Lateral (V/L) means the ratio of the growth rate toward [110] direction to that toward [001] or [001]. As can be seen in Fig. 3.4 (a), V/L of InGaAs increases with decreasing the V/III ratio though it does not change as abruptly as V/L of GaAs. In the case of GaAs, the growth rate for (111) A direction strongly depends on V/III ratio (or AsH_3 pressure)[69, 70]. This is because the (111)A surface of GaAs is terminated by Ga atoms while the (110) surface is terminated by equal numbers of Ga and As atoms. On the other hand, V/L ratio was less sensitive to V/III ratio in the case of InGaAs. With regard to In composition, V/L ration increased with decreasing In mole fraction. From the above results, it is considered that In atoms terminating (111)A surfaces may promote adherence coefficiency of As atoms. It was also found that the temperature has little influence on the V/L of InGaAs. The absolute growth rate increases but V/L ratio was almost independent of growth temperature in the case of InGaAs.

3.2.4 Growth condition and grown structure

On the basis of the results in Section 3.2.2 and 3.2.3, we grew the sample under the condition that the V/III ratio is 20, In content is 0.1, and the growth temperature is 600°C. These results indicate that low V/III ratio and low In composition are desirable to achieve the above structure. The growth pressure was 76 Torr.

Figure 3.4 (a) is the scanning electron microscope (SEM) image of the cross section of the sample. The GaAs layers were selectively etched in order to observe both of the GaAs-InGaAs and GaAs-AlGaAs interfaces. As seen in the micrograph, the InGaAs QWR is formed successfully on top of the GaAs trapezoid. Figure 3.4 (b) shows an atomic force microscope (AFM) image of selectively grown InGaAs QWR structures (before the growth of a GaAs cap layer). As shown in this figure, the InGaAs (GaAs) triangular prisms are formed with very good uniformity.

3.3 Photoluminescence Measurements

μ-PL measurements were carried out with Ti:Sapphire laser pulse (760 nm, 76 MHz). The experimental setup was depicted in Fig. 3.5. The laser beam was focused onto the sample by a microscope objective lens. PL spectra from the sample were transferred to a spectrometer or a charge coupled device (CCD) camera by using the same objective lens. The beam diameter was around 1 mm that equal to the spatial resolution of the present measurement system. The laser beam shape and the size were checked by monitoring the reflection image with the CCD camera. The sample was cooled down to 15 K in a cryostat by a closed cycle helium refrigerator in which vibration and drift was carefully reduced. Spatial images of PL spectra were taken with the CCD camera through band-pass filters corresponding to each of the PL spectral lines.

Figure 3.6 shows PL spectra of the sample. The lateral width of the QWR is about 25 nm. A PL peak at 1.42 eV originates from the InGaAs QWRs, while that at around 1.33 eV from an InGaAs quantum well (QWL) grown on the GaAs substrate (there is no superlattice) at the same time that the InGaAs QWRs were grown. In Fig. 3.6 (a), the photon energy of PL from QWL at position B is slightly different from that at position C. The reason is that the thickness of the QWL at position B is thicker than that at position C due to the diffusion of Ga and In materials from the mask region. The spectral line width of the PL peak from the InGaAs QWRs is about 22 meV. At position B, two peaks were observed because both the InGaAs QWRs and QWL were excited at the same time. Figure 3.6 (b) shows a polarization

dependence of PL from the QWRs at position A (only the QWRs were excited). The strong polarization parallel to the QWRs gives a clear evidence for the carrier confinement to the QWRs. The ratio of peak intensity parallel to the QWRs ($I_{//}$) to that perpendicular to the QWRs ($I_{\perp}$) is 0.38. It should be noted that even in the case of QWL, there is the anisotropic polarization dependence[71]. It was reported that signal ratio $I_{//}/I_{\perp}$ of QWL was 0.6. Therefore, we can conclude that this anisotropy ($I_{//}/I_{\perp}$=0.38) originates from the QWR effects.

3.4 Spatially Resolved Photoluminescence Measurements

Figure 3.7 shows spatial m-PL images of the InGaAs QWRs (λ=870 nm, 1.43 eV), QWL (λ=890 nm, 1.39 eV). The PL image of QWRs shows anisotropic carrier diffusion along the wire direction, while the PL image of QWL shows isotropic expansion. This anisotropic PL distribution along the wire direction is considered to be caused by anisotropic diffusion of excitons in the QWRs. The laser diameter of laser light is smaller than the diffusion length of excitons, PL image should directly indicate behavior of exciton diffusion because observed distribution of PL intensity is corresponding to exciton density. This result is consistent with μ-PL measurement of GaAs QWRs[72]. The influence of the carrier diffusion in the GaAs layer of the superlattice may be included in this anisotropic distribution because there were GaAs layers just under the InGaAs QWRs. However, the PL from the QWRs was identified by spatially resolved PL measurement.

Although the spot size of a laser beam was 1-2 μm, the carrier diffusion perpendicular to the QWRs was observed. This is due to the carrier diffusion in the GaAs cap layer.

Figure 3.8 shows the intensity profiles of photo-luminescence image parallel to the QWRs. The intensity profile shows the exponential decay. At excitation power of 2.2 mW, a diffusion length was approximately 2.75 μm. Here, the diffusion length is defined as a distance between an excited position and a position where PL intensity decreases down to 1/e as large as that the excited position. This value is 1 μm shorter than that in the experiments by Nagamune *et al*[72].

3.5. Concluding Remarks

In Chapter 3, we discussed the fabrication of ridge-type InGaAs QWR structures (lateral width is about 25 nm) on a (110) cleaved plane of AlGaAs/GaAs superlattice by using selective growth. Spatially resolved PL of the QWRs were observed for the first time by using m-PL measurements at low temperature, showing its polarization dependence.

We also observed spatial μ-PL images of carrier diffusion in the InGaAs QWRs, showing anisotropic PL distribution along the wire.

The FWHM of PL peak of the QWRs was a little broad compared with the V-shaped QWRs in spite of good uniformity of mask patterns. Growth condition needs more optimization in order to better quality of QWRs.

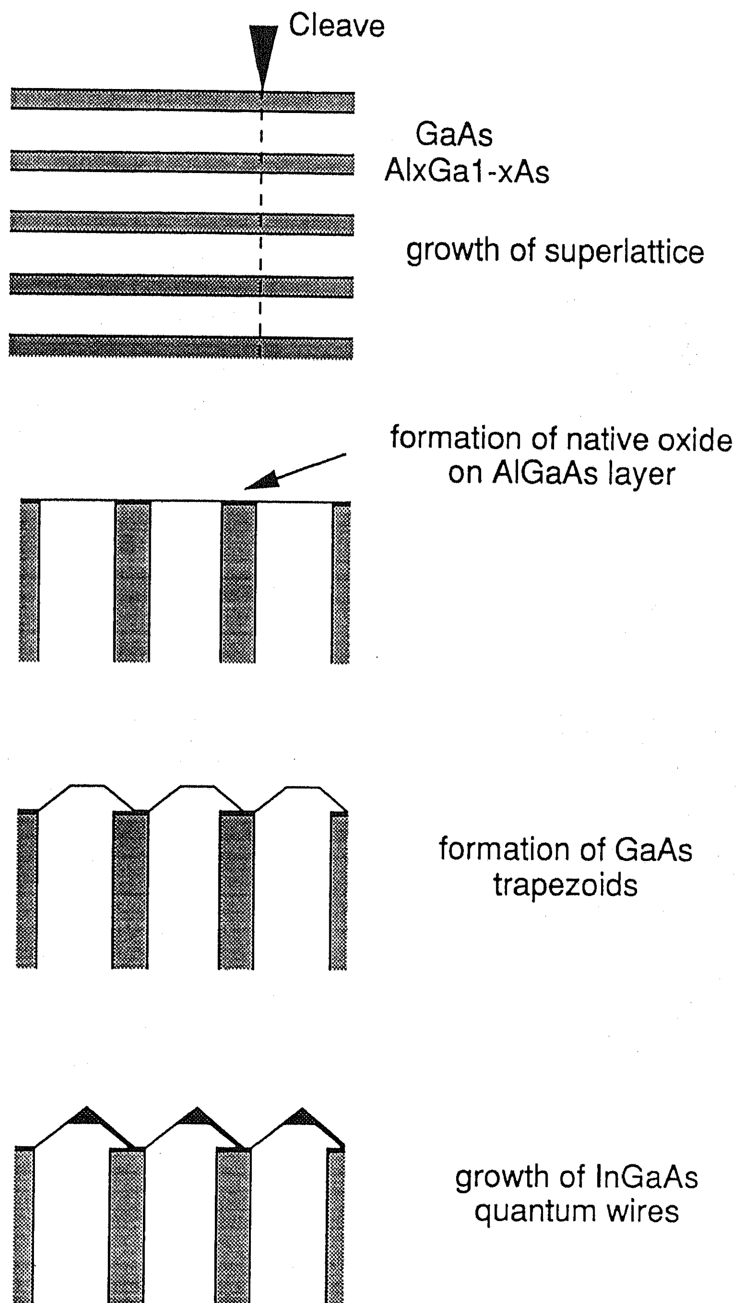

Fig. 3.1 Fabrication process ridge-type InGaAs quantum wires.

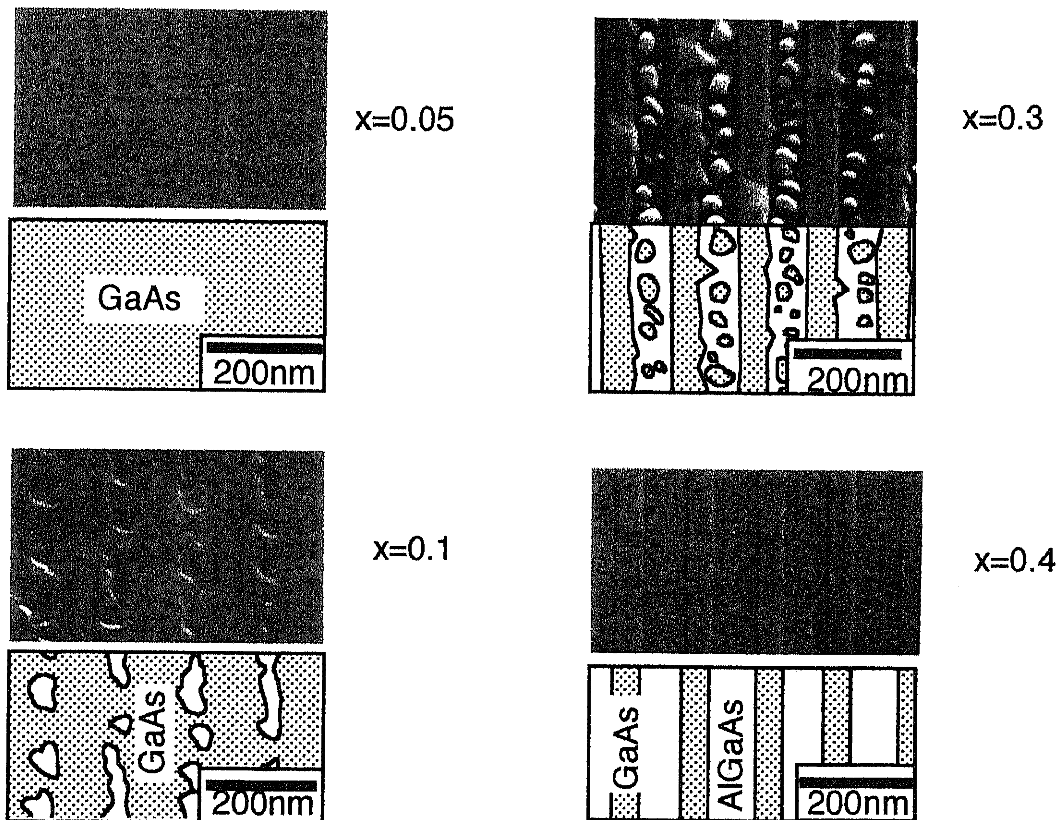

Fig.3.2 Scanning electron microscope images and schematic illsutration of the GaAs on a cleaved (110) facet of AlAs/ $Al_xGa_{1-x}As$ superlattice

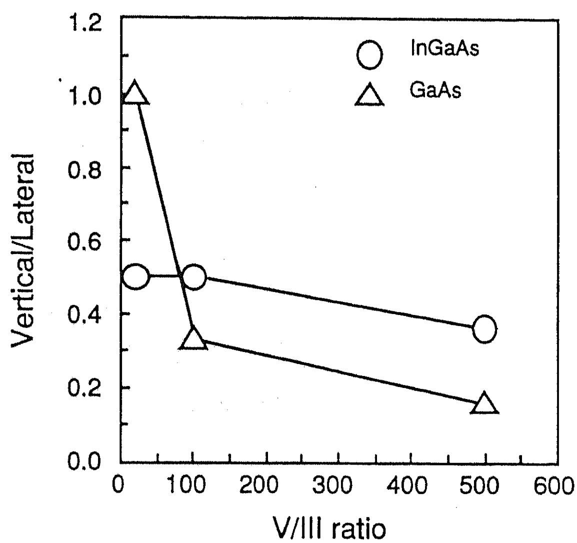

(a)

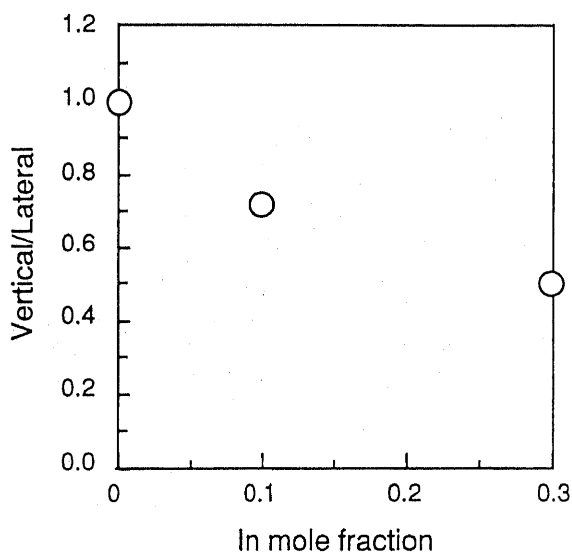

(b)

Fig. 3.3 Growth rate dependence of InGaAs layer on (a) V/III ratio, (b) Indium composition. In Fig .3.3 (a), In mole fraction is 0.3. The growth pressure and temperature is fixed at 76 torr and 600 °C, respectively. The vertical axis Vertical/Lateral (V/L) means the ratio of the growth rate toward [110] direction to that toward [001] or [001].

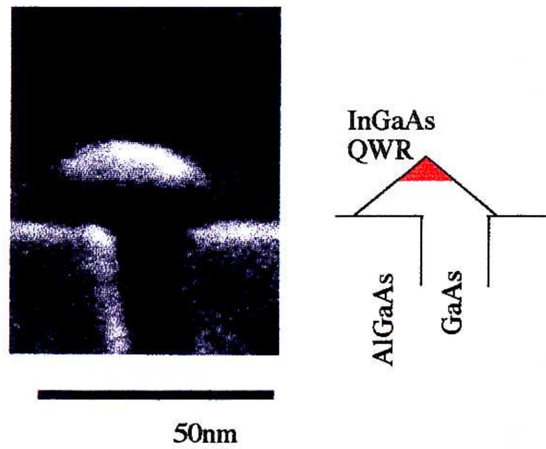

(a)

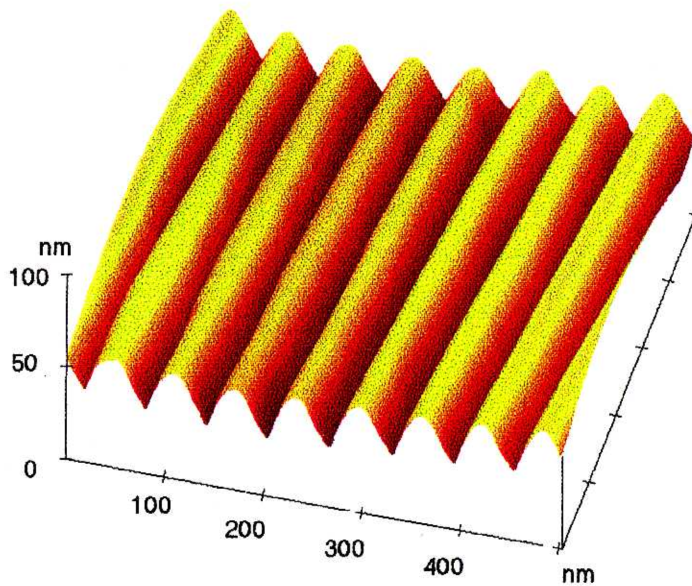

(b)

Fig. 3.4 (a) A scanning electron microscope (SEM) image of the cross section of the sample. The GaAs layers were selectively etched. (b) An atomic force microscope (AFM) image of selectively grown InGaAs QWR structures (before the growth of a GaAs cap layer).

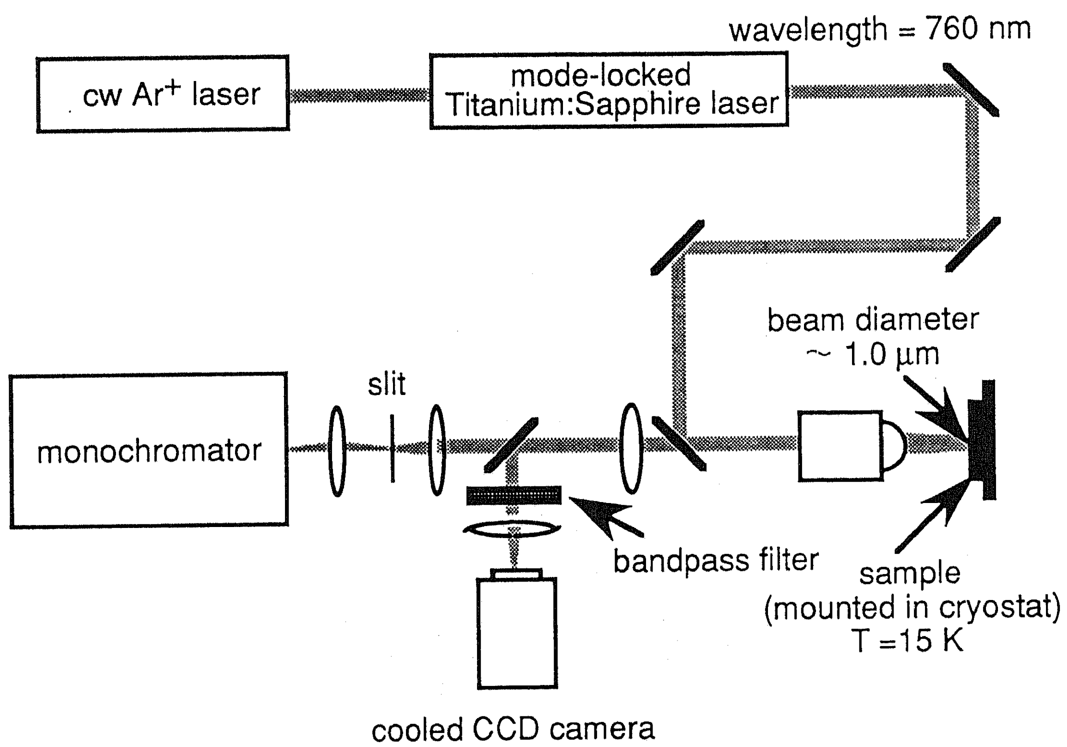

Fig. 3.5 Micro-PL measurement setup.

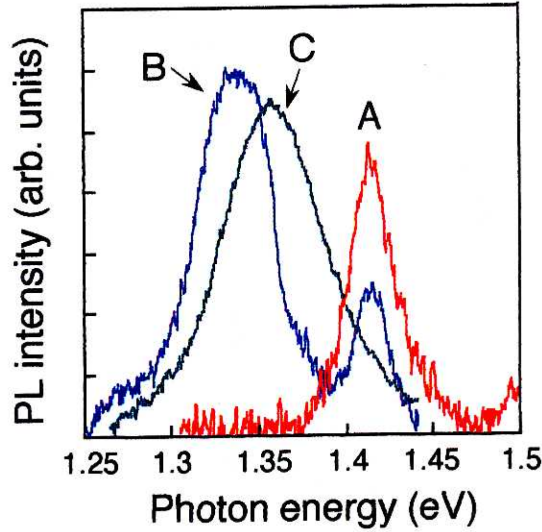

(a)

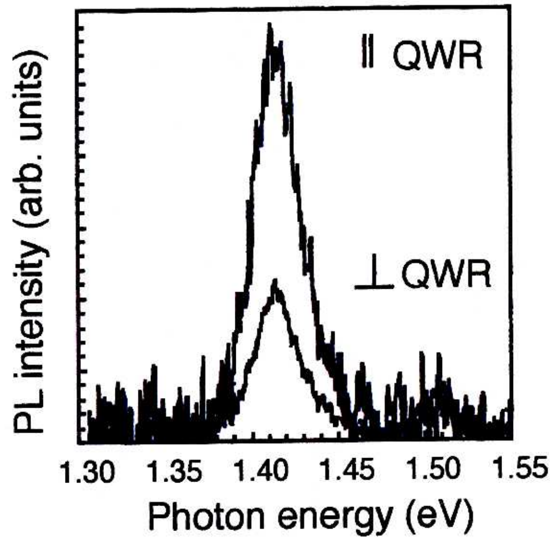

(b)

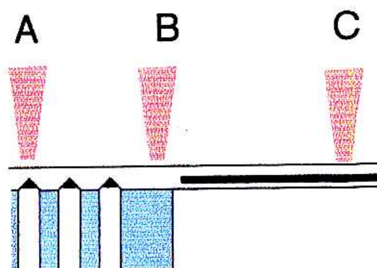

(c)

Fig. 3.6 (a) PL spectra of the sample at position 1 (only QWRs were excited), position 2 (both QWR and QWL were excited), and at position 3 (only QWL was excited). (b) Polarization dependence of PL form the QWRs at position 1. (c) Schematic illustration of the excited positions.

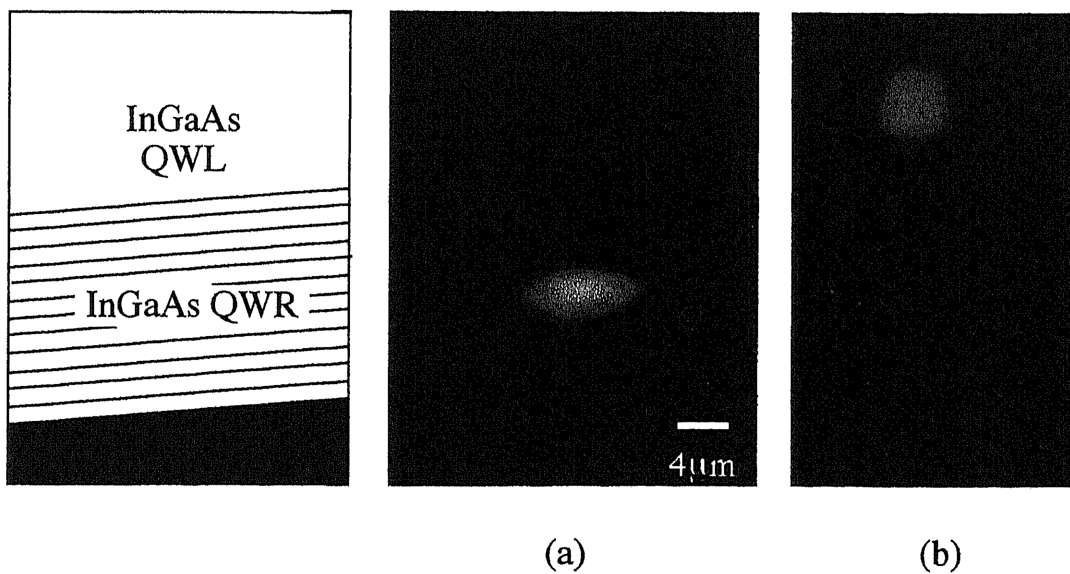

Fig. 3.7 Spatial μ-PL images of InGaAs QWRs and QWL. (a) μ-PL image at λ=870nm (InGaAs QWRs), showing anisotropic carrier diffusion along the wire direction. (b) μ-PL image at λ=890 nm (InGaAs QWL), showing isotropic expansion.

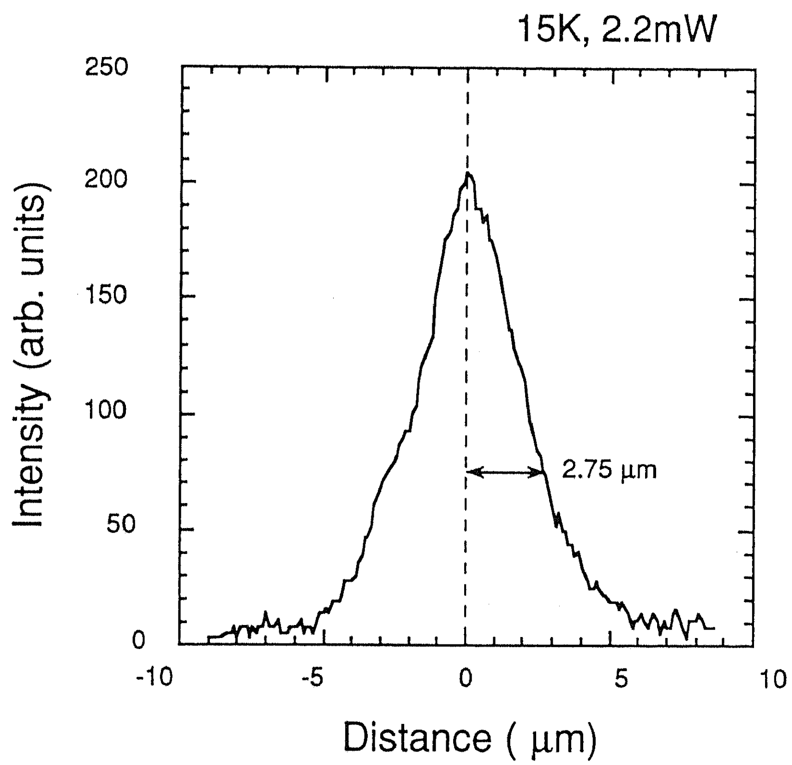

Fig.3.8 Intensity profile of photoluminescence image parallel to the InGaAs QWRs.

Chapter 4

Fabrication of Microcavity Quantum Wire Lasers

4.1 Introduction

As discussed in Chapter 2, we succeeded in fabricating GaAs and InGaAs quantum wires (QWRs) of high quality. In this structure, the QWR effects were clearly demonstrated with photoluminescence (PL) and photoluminescence excitation (PLE), magneto-PL measurement[73]. On the other hand, vertical-cavity surface-emitting lasers (VCSEL) have received great attention for light sources in optical communication, optical signal processing, and optical computing of the next generation[74, 75]. Moreover, the use of microcavity structures is expected to achieve substantial reduction of the threshold current due to the controlled spontaneous emission mode[76, 77]. Strong interactions between excitons (or zero-dimensional electrons) and photons in the microcavity bring important phenomena including Vacuum Rabi Oscillation[78]. Thus the control of both photon modes and electron modes in confined structures is important for the ultimate light sources[79].

The first demonstration of QWR microcavity lasers were reported by reported by Chavez-Pirson *et at.*[80] They fabricated the QWR laser structure using GaAs/AlAs fractional layer superlattice (FLS). The FLS growth method can produce high density QWR

arrays, however, there are some problems in uniformity and lateral confinement as QWRs.

In this chapter, as a step toward the ultimate lasers, we demonstrate the fabrication of a strained quantum wire laser with a vertical microcavity based on this previously established technology described in Chapter 2. First, we demonstrate the fabrication process of the laser structures which consist of a cavity with an optical length of 4 λ or 2 λ (λ: emission wavelength) and AlAs/AlGaAs distributed Bragg reflectors (DBRs). Second, we discuss the optical characteristics of the 4λ-microcavity lasers.

4.2 Fabrication of Microcavity Laser Structures

4.2.1 Fabrication process of 4 λ-microcavity lasers

Figure 4.1 shows the fabrication process of the laser structure. In the microcavity, triangular-shaped $In_{0.3}Ga_{0.7}As$ strained QWRs are grown between (111)A facets of [0-11]-oriented GaAs triangular prisms by selective MOCVD growth on a SiO_2 masked DBR mirror region. The QWRs are compressively strained owing to the difference of the lattice constants of GaAs (or AlGaAs) and $In_{0.3}Ga_{0.7}As$. A scanning electron micrograph and a schematic illustration of the cross section of the laser structure are shown in Fig. 4.2. The top and bottom DBRs consist of 25 and 30.5 quarter-wave pairs of $Al_{0.4}Ga_{0.6}As$/AlAs, respectively. To obtain an upper DBR of high quality, the region above the quantum wires must be flat. Therefore, the quantum wires were buried with GaAs, instead of AlGaAs. Since the diffusion length of Ga is larger than that of Al, the growth of GaAs can flatten the uneven surface left after the quantum wire growth. In order to use GaAs as the barrier region on the quantum wires, InGaAs material of which the bandgap is smaller than that of GaAs was grown as the quantum wire region. In addition, the use of the strain effects in the quantum wire leads to substantial improvements in lasing characteristics [42, 81].

The growth process of the $In_{0.3}Ga_{0.7}As$ strained QWR region is the same as that reviewed in Chapter 2. The lateral width of the QWR was about 10 nm. The period of QWR was 200 nm. To increase the interaction between excitons and photons, the QWRs should be located

at the antinode where the standing wave of the electric field in the cavity has a peak. Therefore, the laser structure was designed as shown in Fig. 4.2. The material-cavity interaction becomes very strong as the cavity length is reduced to the dimensions comparable to emission wavelength. Therefore, shorter cavity length is better for realizing highly efficient lasers. However, it is not easy to obtain flat cavity surface when the shorter cavity length. Therefore, the cavity length was designed to be 4 λ as the first step to the lasers with the novel structure.

4.2.2 Fabrication process of 2 λ-microcavity lasers

The material-cavity interaction becomes very strong as the cavity length is reduced to the dimensions comparable to emission wavelength. Therefore, shorter cavity length is better for realizing highly efficient lasers.

The major obstacle for the realization of the laser structure discussed in this chapter with shorter cavity length is the difficulty of fabricating an upper DBR of high quality. To obtain good upper DBRs, it is very important to make the interface between the cavity spacer and the DBR very smooth. In the case of 4 λ-cavity, we could obtain upper DBR of good quality because flattening the surface above the QWRs was not so difficult due to the long GaAs spacer. However, the shorter the cavity length is, the more difficult it becomes to achieve the flatness of the surface. Hence, the growth condition should be optimized.

On the other hand, the photons were not confined laterally in the above planar-type structure. In actual VCSELs, sidewalls are usually formed by introducing buried heterostructures or by dry etching techniques to make airposts with a few micron diameter[82], obtaining large photon confinement. In our structure, the grating was formed in the lateral direction and the QWRs were periodically located. Therefore, if the period is optimized , gain-coupled or index-coupled laser structures, which confine the photons in the lateral direction, can be realized.

In this section, we discuss the improved growth condition for realizing 2λ-microcavity structures and the lasing characteristics.

In order to obtain a flat surface of the spacer layer above the active region, we modified the growth condition. Figure 4.3 shows the modified growth sequence. The upper spacer layers (and DBRs) were grown at higher temperature (750 °C) and lower V/III ratio (~20), slower growth rate (0.27 nm/sec), resulting in longer migration lengths of Ga atoms. Al composition of AlGaAs layers in the top DBRs was decreased to 0.2. The surface flatness was improved as shown in Fig. 4.4. It is also important to make line patterns without defect. If there are some defects, flat surfaces cannot be obtained even by growing under the improved growth condition.

4.3 Optical Characteristics of Microcavity Lasers

In this section, we discuss the optical properties of 4 λ-microcavity lasers.

4.3.1 Photoluminescence of AlGaAs/InGaAs/GaAs quantum wires without a cavity

The AlGaAs/InGaAs/GaAs QWRs are used for the microcavity lasers and their optical properties are different from the AlGaAs/InGaAs/AlGaAs QWRs. Figure 4.5 shows the PL spectra of the AlGaAs/ $In_{0.3}Ga_{0.7}As$ /GaAs QWRs (without the cavity). Some distinctive features can be seen compared with the AlGaAs /InGaAs/AlGaAs QWRs discussed in Chapter 2. The emission of the QWRs is relatively much stronger than that of the QWLs on sidewalls. This is because carriers in the QWL easily escape into the GaAs barrier being different from the case of AlGaAs barriers. The emission energy of the QWRs is a little lower than that with AlGaAs upper barrier layers due to reduced carrier confinement. The peak width is slightly narrower because there is no fluctuation of Al composition in upper barrier layers resulting in reduction of potential fluctuation of the QWRs.

4.3.2 Photoluminescence of QWR laser structure with a cavity

Figure 4.6 (a) shows the reflectivity and PL spectrum of the sample (4 λ cavity) measured at 14K. The reflectivity spectrum of the sample was measured using white light. The cavity resonance was designed so that the resonance photon energy coincides with the PL peak of the quantum wires. As shown in this figure, a sharp PL spectral line with a full width at half-maximum (FWHM) of less than 3 nm was observed from the quantum wires with the cavity. On the other hand, the FWHM of the PL spectra from the quantum wires without the cavity was about 16 nm (Fig. 4.6(b)). The narrowing of spectrum due to the cavity clearly demonstrates the cavity effect.

Figure 4.7 shows the PL spectra polarized parallel to the QWRs and that perpendicular to the QWRs. As seen in the figure, the PL showed the clear polarization dependence, indicating the QWR effects.

4.3.3 Lasing characteristics of QWR lasers

The lasing properties of this sample were measured at 77K, using optical pumping with a continuous wave Ti:Sapphire laser with the wavelength of 733 nm. Figure 4.8 shows the output power of the light emitted from the sample as a function of pumping laser power. The beam diameter of the pump beam was about 200 μm. The measurement showed a clear threshold at a pump power of ~40 mW, demonstrating lasing oscillation at this temperature. This result demonstrates the possibility of extremely low threshold current, less than 100 μA by reducing the diameter of the cavity down to 1 μm.

Even above the threshold, the width of the spectra is rather broad. The reason can be explained as follows. There are many lasers with various emission wavelength due to the wide excited area.

In order to confirm the lasing oscillation, we performed time resolved measurements. Figure 4.9 displays time trace of the emission from the 4λ-cavity laser above the threshold (excited at 60 mW). The sample was excited by the same Ti:sapphire laser pulse. The pulse width of the emission from the QWR laser was about 200 ps (FWHM). This value is rather large as a laser oscillation. The upper mirror of the microcavity is imperfect even in the case of 4λ cavity. When the optically pumped area is large, multiple lasing[83] will occur. This means the observed lasing characteristics is that of a mixture of the lasers with different characteristics. Therefore, the pulse width is large in spite of lasing.

4.4 Concluding Remarks

In Chapter 4, a vertical microcavity InGaAs strained QWR lasers were investigated using MOCVD selective growth as a step toward the ultimate lasers.

Fabrication process of the 4λ- and 2λ-cavity laser structures were discussed and the problems in fabrication were revealed. In particular, flattening the spacer layer above the QWRs are important.

With respect to the 4λ-cavity lasers, optical characteristics were investigated. The cavity effect was evidenced by the difference of the PL broadening with and without the cavity. Lasing was observed at 77K by using optical pumping. The threshold input power was very low and the feasibility of the QWRs for laser diodes was demonstrated. The lasing oscillation was confirmed by time resolved measurements.

Unfortunately, we have not obtained lasing from 2λ-microcavity lasers yet. Further work is needed in order to realize 2λ-microcavity lasers.

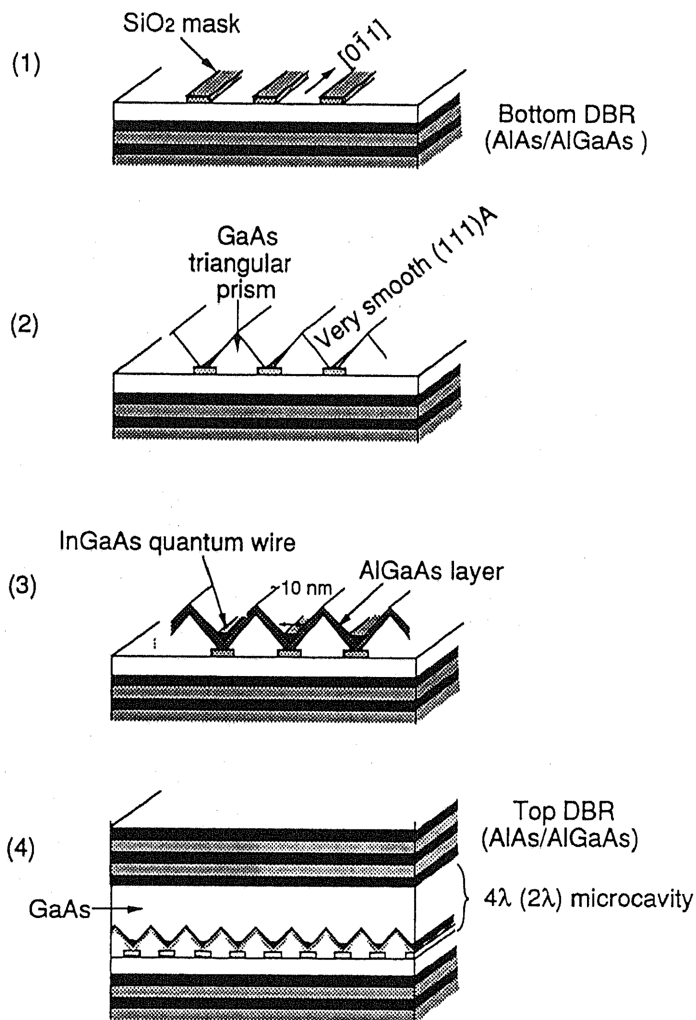

Fig. 4.1 Fabrication process of the microcavity quanum wire laser structure using selective MOCVD growth technique.

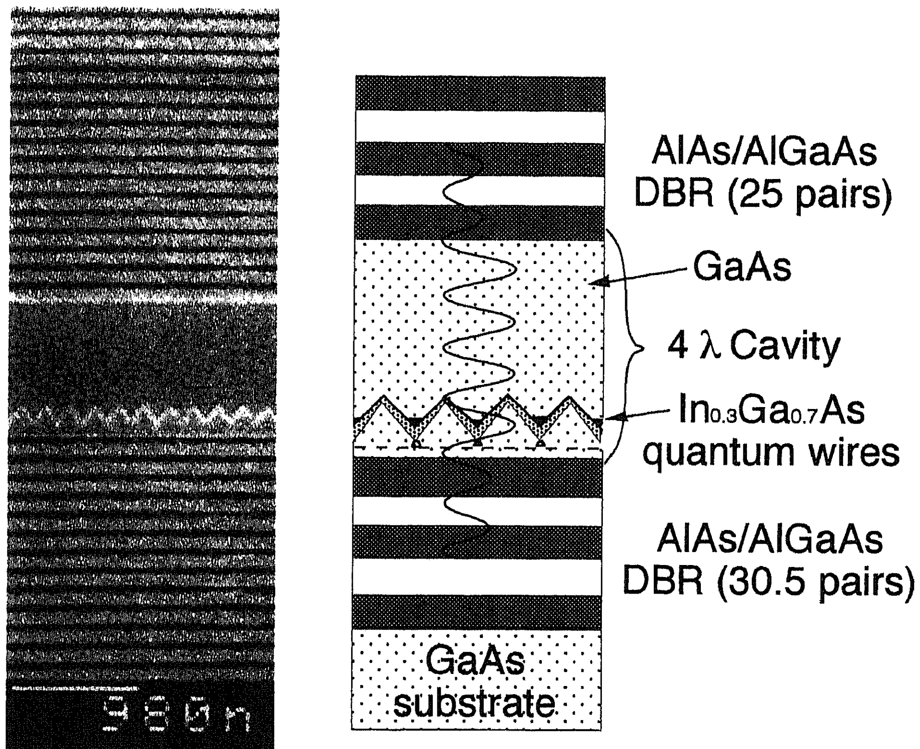

Fig. 4.2 A schematic illustration and a scanning electron micrograph of the laser structure(4λ-cavity).

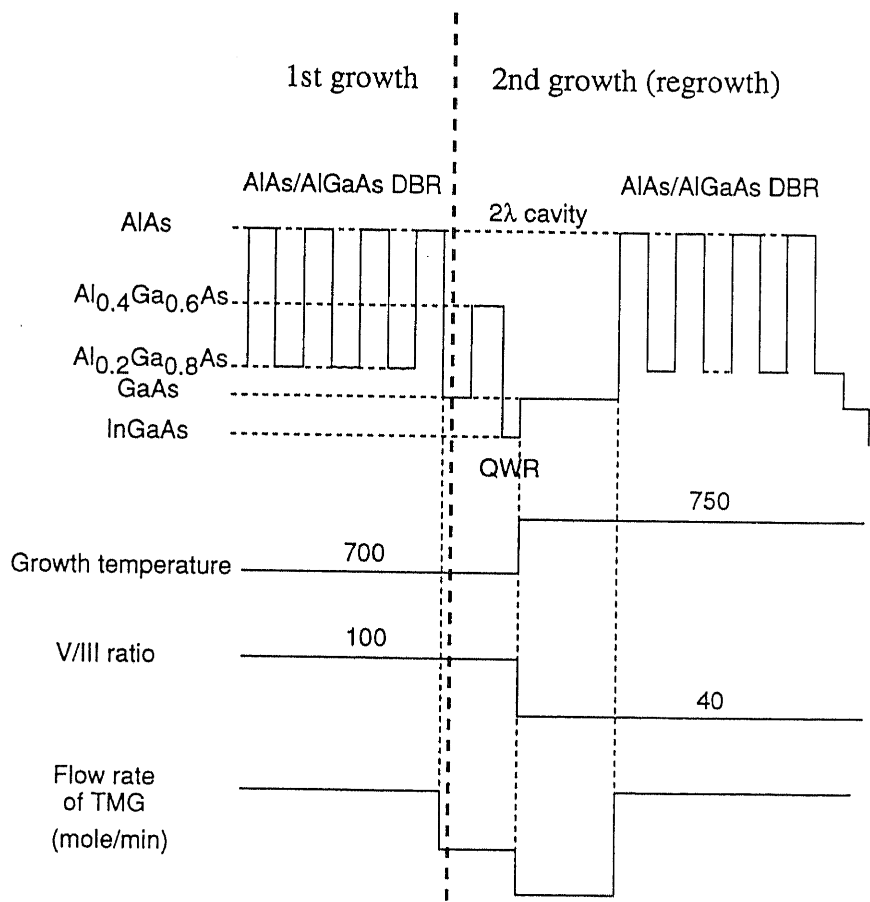

Fig4.3 Modified growth sequence for 2 λ-cavity QWR laser structure

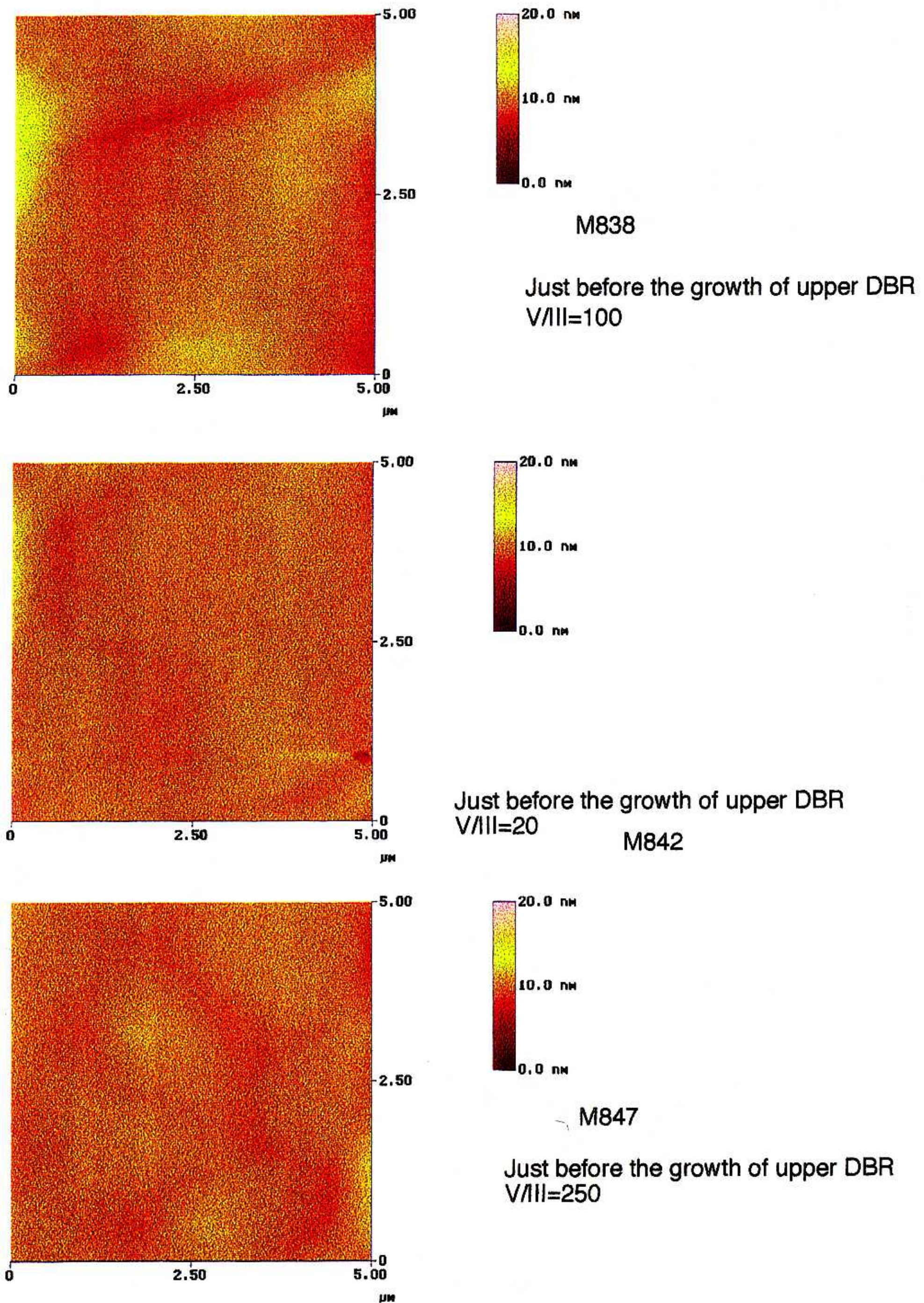

Fig. 4.4 AFM images of the upper GaAs spacer layers grown under various V/III ratios.

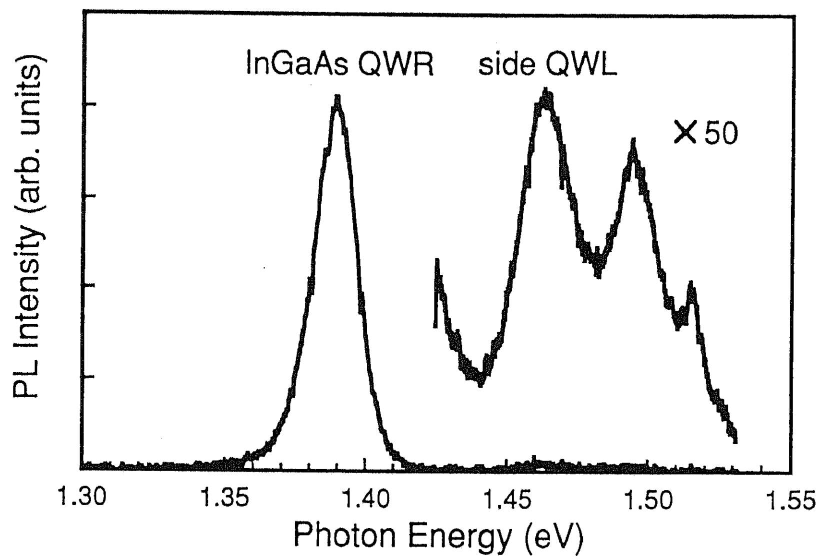

Fig. 4.5 PL spectra of the AlGaAs /$In_{0.3}Ga_{0.7}As$ /GaAs QWRs without the cavity.

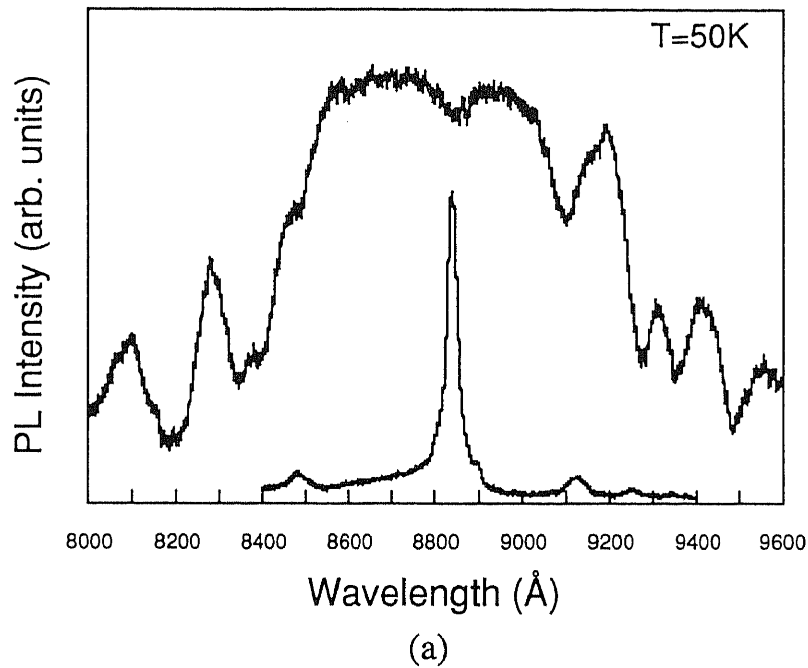

(a)

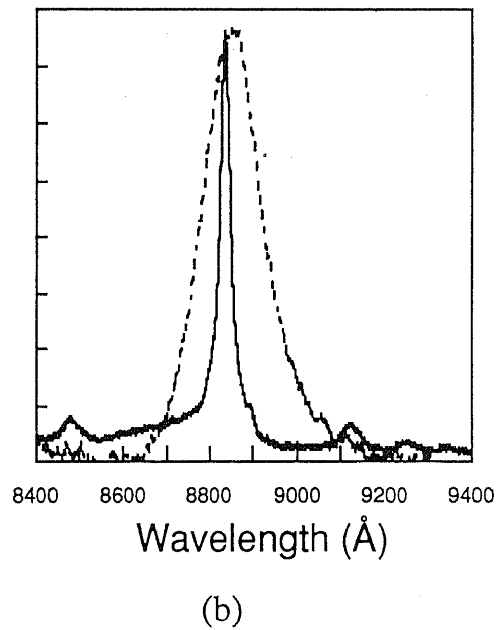

(b)

Fig. 4.6. (a) The upper curve is reflectivity spectrum of the sample. The lower curve is PL spectrum of the sample with the cavity. (b) PL from the QWRs with and without the cavity.

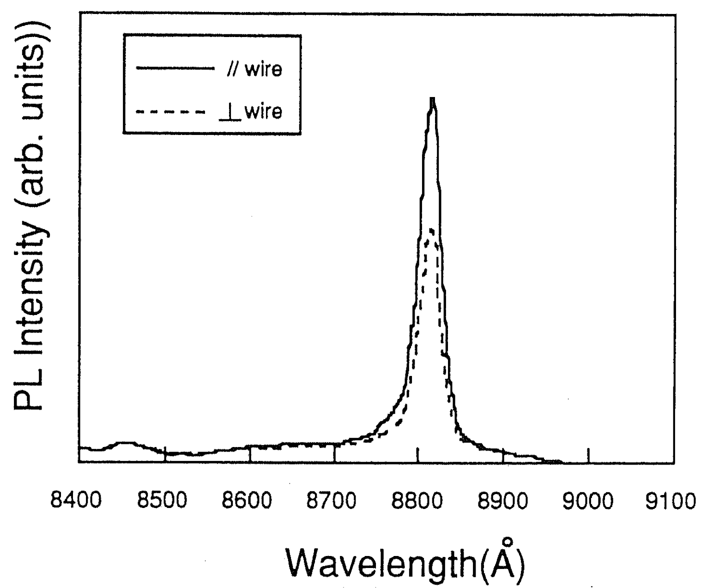

Fig. 4.7 PL spectra polarized parallel to the QWRs and that perpendicular to the QWRs.

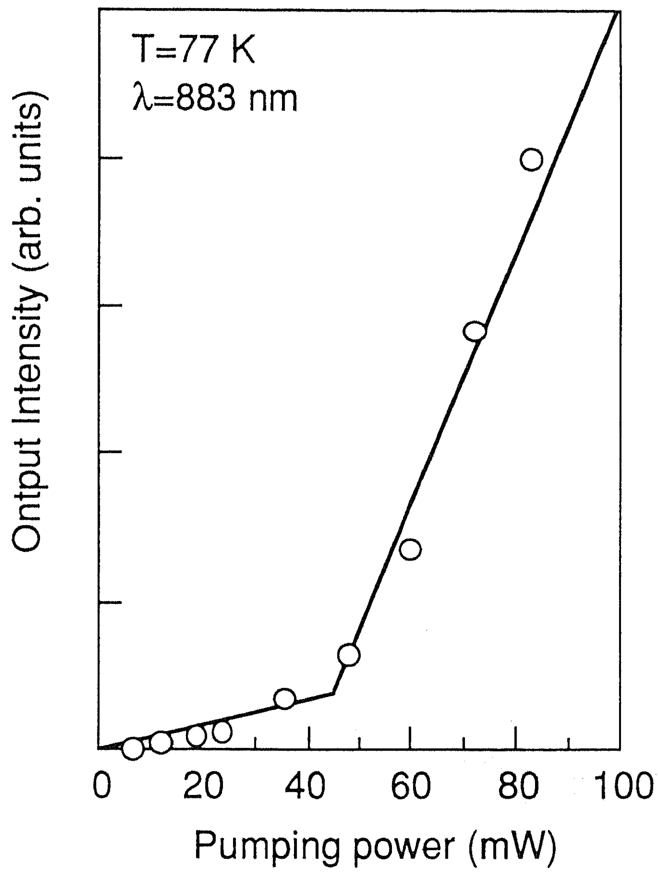

Fig. 4.8 Light output intensity from the sample as a function of pumping laser power.

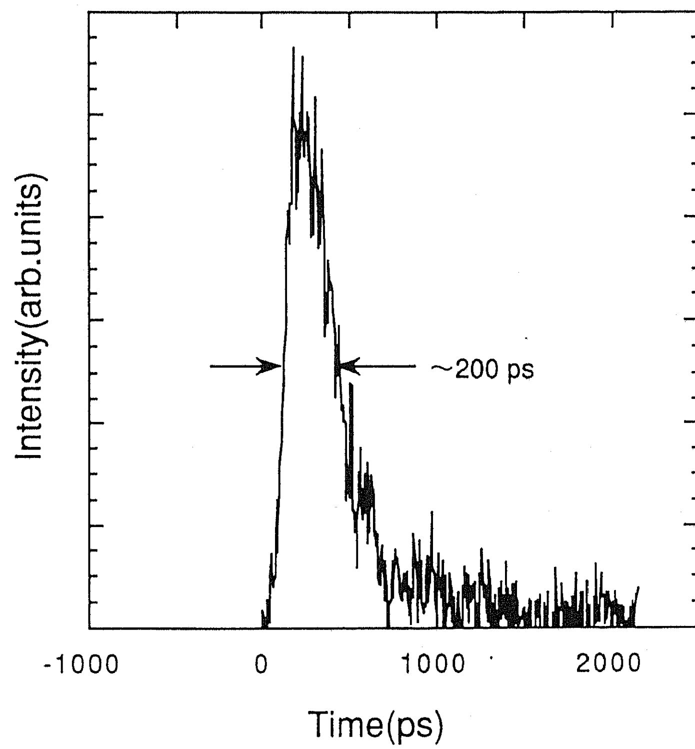

Fig. 4.9 Time trace of the emission form the 4l-cavity laser above the threshold.

Chapter 5

Quantum Confined Stark Effect in GaAs Quantum Wires

5.1 Introduction

Electric fields applied perpendicularly to the layers of quantum wells significantly change the optical absorption, reflection, and photoluminescence properties. This effect is referred to as the quantum confined Stark effect (QCSE) and has been first measured by Wood *et al.* as changes in absorption spectra of GaAs/AlGaAs multiple quantum wells[84-86]. Since changes in the optical absorption can be employed for optoelectric modulators, the QCSE is very promising for the realization of fast optical switches, modulators, self-electro-optic effect devices (SEEDs)[87], and so on. The QCSE in quantum wires and quantum dots is also of great interest because a large oscillator strength due to enhanced excitonic effects is expected in such structures. This feature is important for applications of the nanostructures to optical modulators with lower voltage operation and ultrafast switching times. It was also predicted that electroabsorption is enhanced in the quantum wires and quantum dots owing to the enhanced oscillator strength[2]. Therefore, such nanostructures are promising for low energy optoelectronic devices.

There are a few reports on the experiments. For example, Schilling *et al.* investigated the QCSE in InGaAs/InP quantum wires

fabricated by we chemical etching[88]. They observed a normal red shift up to 25 meV with the intensity of the photoluminescence decreasing similar to effectively 2D structures. The width of their QWR is very large (85 nm), resulting in small lateral confinement. The behavior was similar to the QCSE in QWLs. Rinaldi *et al.* also investigated the QCSE in InGaAs/GaAs quantum wires[57]. They observed that PL spectra exhibit a small blue shift due to a internal piezoelectric field caused by strain in QWRs.

In this chapter, we investigate the QCSE in the GaAs quantum wires experimentally, demonstrating observation of a clear blue shift of the photoluminescence peak with the increase of electric fields. This is considered due to the enhanced binding energies of excitons in nano-structures. Time-resolved PL measurements were also performed. The PL decay times are decreased in narrow quantum wires (lateral width L_x =8 nm) with the increase of electric fields, while the decay times are increased in wide quantum wires (L_x=35 nm).

5.2 Sample Structure

Schematic illustrations and a scanning electron microscope image of the sample used in the experiments are shown in Fig. 5.1 The quantum wires were grown in a V-groove structure[50]. The feature of the growth technique developed previously by our group is that the V-groove is formed epitaxialy by the selective growth technique[25]. The GaAs quantum wire structures were grown using the selective growth on SiO_2 patterned GaAs (100) substrate with low pressure metal organic chemical vapor deposition (MOCVD). Using this technique, we obtained quantum wires with a lateral width of less than 10 nm in 1993 [49]as mentioned in Chapter 2.

The structure consists of Si-doped 50 nm-thick n^+-type $Al_{0.4}Ga_{0.6}As$, undoped 50 nm-thick $Al_{0.4}Ga_{0.6}As$, undoped GaAs quantum wires, undoped $Al_{0.4}Ga_{0.6}As$, and an undoped GaAs cap layer. The detailed growth procedure of the quantum wire structure is described elsewhere[25]. A semitransparent Schottky contact (Ti/Au, 100/50Å) and an ohmic contact (AuGe/Ni/Au) were evaporated on the front and the back sides of the sample, respectively. Penetration rate of the semitransparent contact was about 30% in an Ar^+ laser (λ=514.5 nm). Si was doped up to the middle of AlGaAs layer under GaAs quantum wires ($n=4\times10^{18}$ cm^{-3}) in order to avoid the influence of SiO_2 masks on an electric field. The electric field perpendicular to the quantum wire layer was applied with a dc bias voltage between the n^+ substrate and the Schottky barrier.

5.3 Photoluminescence Measurements

PL was measured at 50 K with an Ar^+ laser (λ=514.5 nm). The excitation power (P_{ex}) was 0.26 Wcm^{-2}. Figure 5.2 shows the dependence of PL spectra on the externally applied voltage V_{ext}. Lateral width (L_x) of the quantum wire is (a) 8 nm, (b) 35 nm, respectively. The flat band voltage of the sample, corresponding to zero current flow, was measured to be about 0.6V. PL from the quantum wires (nm) was observed at 1.680 eV as shown in Fig. 5.2 (a). In Fig. 5.2 (b), the peaks at 1.530 eV and 1.607 eV correspond to PL from the quantum wires and the quantum well regions on (111)A facet of AlGaAs layers, respectively. A shoulder peak at around 1.553 eV can be also observed, which can be attributed to arrow-head shaped quantum wires[48]. Figure 5.3 shows the PL peak position of the quantum wires as a function of V_{ext} and the electric field E_{ext}. Here, the electric fields in the quantum wire structures were calculated with the finite element method (FEM) with taking the dielectric constants of GaAs and AlGaAs into account (Fig. 5.4). As a reference, peak positions of photoluminescence from GaAs quantum well (100Å) are also plotted. In the case of L_x=35 nm, the PL spectra show a red shift, as observed in conventional GaAs quantum wells. On the other hand, the quantum wires of smaller lateral size (L_x=8, 14 nm) exhibit a small but clear blue shift when V_{ext} is less than 0.3 V. The blue shift as large as 7.93 meV are obtained in the case of L_x=8 nm, and 4.83 meV in the case of L_x=14 nm. The luminescence energy from the quantum wires does not shift at all, but its intensity decreases rapidly with increasing field.

The QCSE in quantum wires was also experimentally investigated by Rinaldi *et al.* [57]. They also observed a small blue shift of PL of the order of 2 meV in InGaAs/GaAs quantum wires. In their experiment, quenching of PL from the quantum wires was observed in each case of forward and reverse biases. The blue shift was considered to be due to the piezoelectric field caused by the strain in the quantum wires. On the other hand, the quenching effect was not observed in a reverse bias in our experiments. This indicates that our results are different from the phenomena observed by Rinaldi *et al.*

If the external electric field E_{ext} is not perpendicular to the quantum wires, we should consider the effects of different vectorial composition of E_{ext}. We calculated the distribution of E_{ext} in the structure by the FEM. As a result, it was confirmed that the E_{ext} in the quantum wire region is applied in parallel with the growth direction as shown in Fig. 5.4. In addition, the wavefunction of the ground state is concentrated on the center of the quantum wire structures. Therefore, we do not need to consider such effects.

The blue shift observed in our experiment can be understood by considering enhanced binding energy E_b of excitons in the quantum wires. When the electric field E_{ext} is applied to the quantum wells, the red shift of the PL peak is observed owing to the following relation.

$$E_b(0) - E_b(E_{ext}) < E_q(0) - E_q(E_{ext}), \qquad (1)$$

where $E_b(E)$ and $E_q(E)$ are the binding energy of excitons and quantized energies of electrons and holes without considering the excitonic effect. On the other hand, in narrower quantum wires,

$E_b(E)$ drastically decreases function of the electric field, because the binding energy with the zero-electric field is very large. As a result, in the range of the electric field form the zero-field to a certain value E_o, the following relation must be satisfied.

$$E_b(0) - E_b(E_{ext}) > E_q(0) - E_q(E_{ext}). \quad (0 < E_{ext} < E_o) \quad (2)$$

This relation clearly leads to the blue shift of the PL peak in the quantum wires. Since the binding energy is not so high in wider quantum wires, there is not E_{ext} which satisfies the Eq. (2). The above interpretation is supported by the calculated results by Benner *et al.* [89] In our experiments, The smaller the dimension of the quantum wire is, the larger the binding energy of excitons becomes. Therefore, the result that the value of the blue shift in smaller quantum wires (L_x=8 nm) is larger than that in wider quantum wires (L_X=14 nm) is consistent with the above explanation.

A similar blue shift (7 meV) was observed in InGaAs quantum dots grown in the Stranski-Krastanow growth mode by MOCVD[90].

For the SEEDs, a blue-shifting diode has important consequences[91]. In normal red-shifting quantum well diodes, the exciton peak red-shifts upon bias and the absorption decrease. However, large residual absorption remains even at very large biases. In a blue-shifting quantum well diodes upon bias, the absorption would decrease to subband-gap values under much smaller biases, which results in lower voltage operation and much less absorption in its transmitting state. In order to realize the blue-shifting quantum well diodes, several structures have been reported[92, 93]. In our quantum

wire structure, we can easily obtain blue shift of exciton peaks. Hence, the QWRs are feasible for the SEEDs.

The V-shaped quantum wires are anisotropic in shape in the growth direction. Therefore, the behavior of PL from the quantum wires should depend on the direction of an electric field. Figure 5.5 shows the PL spectra for the sample with arrow-head shaped QWRs (AH-QWRs) which are formed on top of the triangular prisms. They appears when the lateral width of the quantum wire is in a certain range. The peak at 1.53 eV can be attributed to the additional AH-QWRs The AH-QWRs can be regarded as inverted V-shaped quantum wires. In Fig. 5.5, the three distinct peaks at 1.63, 1.59, and 1.53 eV are attributed to the luminescence from the quantum wells on (111) A, arrowhead quantum wires, V-shaped quantum wires, Si-doped GaAs bulk, respectively. As seen in this figure, the behaviors of the PL peaks are different from each other. Figure 5.6 shows the dependence of PL intensity on the energy shift with respect to two kinds of quantum wires. In the case of the AH-QWRs, the luminescence intensity does not change appreciably in spite of the drastic line shift compared with the V-shaped quantum wires. Their different behaviors can be explained by considering the cross-sectional shapes of the QWRs. When the electric field is applied, the wavefunction of the hole is pressed against the barrier more strongly than that of the electron. Therefore, the state of the hole is dominant in the QCSE. In the case of V-QWRs, the barrier height of the top AlGaAs layer is effectively lower than that of the bottom due to the asymmetrical shape of the cross section and vice versa in the case of AH-QWR. Therefore, the

overlap of the electron and the hole in V-QWR under the same electric field should be smaller than in AH-QWR.

In addition, the peak of the sidewall QWL shows the blue shift due to the tapering of the thickness of the QWL. PL intensity from thicker QWLs quenches faster than that from thinner ones under electric fields. Therefore, it exhibits the blue shift apparently.

5.4 Time Resolved Photoluminescence Measurements

Time-resolved PL measurements were also carried out at 50K using a mode locked yttrium aluminum garnet (YAG) laser (λ=532 nm) with a repetition rate of 82 MHz. PL from the samples was measured using a synchroscan streak camera with a resolution of 7 ps. The total resolution of the system was 20 ps.

Figure 5.7 displays the temporal evolution of the PL peaks associated with the quantum wire transition (L_x=8 nm) at various V_{ext}. The data were normalized at their maximal. As shown in this figure, PL decay time increases with the increase of V_{ext}. PL decay times were plotted as a function of applied voltage at two kinds of excitation powers (P_{ex}=7.8 W/cm^2, 78 W/cm^2) in Fig. 5.8. At ten times higher excitation, PL decay time showed a similar tendency as shown in this figure. In the case of P_{ex}=7.8 W/cm^2, the decay time was independent (440 psec) up to V_{ext} ~ -0.1 V. The decay time decreases with the increase of V_{ext} when Vext is more than -0.1 V. In the case of P_{ex}=78 W/cm^2, the decay time decreases gradually from 550 psec and behaves as well as in the case of P_{ex}=7.8 W/cm^2.

The dependence of PL decay time on the V_{ext} and L_x is depicted in Fig. 5.9. P_{ex} was 78 Wcm^{-2}. The carrier life times of the 8 nm-, 35 nm- quantum wires at the flat band condition were 440 ps, 510 ps, respectively. In the case of L_x=35 nm, the PL decay time is prolonged by V_{ext}. On the other hand, the PL decay time decreases with V_{ext} in the case of L_x=8 nm.

The increase of the PL decay time is considered to be due to spatial separation of the electrons and holes under the electric field.

This separation reduces the electron-hole spatial overlap, increasing of exciton radiative life time. The radiative recombination lifetime τ_r is given by

$$\tau_r = \tau_o / |M_{cv}|^2$$

in the one-particle picture, where M_{cv} is the overlap integral of the electron and hole wave functions[86], and τ_o is the lifetime under flat band condition. The decrease can be explained as quantum mechanical tunneling of electrons and holes through the barriers. These results indicate that the tunneling mechanism dominates reduction of overlap of the wavefunction of electrons and holes when the quantum wire is narrower. This tendency was also observed in quantum wells[94, 95].

5.5 Concluding Remarks

In Chapter 5, the QCSE in the GaAs quantum wires was experimentally investigated. We demonstrated the observation of a blue shift of the PL peak in the GaAs quantum wires with various sizes. We believe this blue shift results from the enhanced excitonic effect due to the strong confinement in the nanostructures. The blue shift results in large absorption change with small absorption wavelength. This feature is suitable for optical modulators. Therefore, the QWR structure is very promising. In order to increase the total change of absorptions, higher density of QWRs requires, for example, by stacking the QWRs.

Time resolved PL measurements were also performed. As a result, we found the recombination lifetime of the exciton emission line depends strongly on the dimension of the quantum wire. That is, the PL decay time decreased in small quantum wires (L_x=8 nm) with the increase of electric fields, while it increased in large quantum wires (L_x=35 nm). This results shows that when the quantum wire is narrower, tunneling mechanism of carriers dominates reduction of overlap of the wavefunction of electrons and holes.

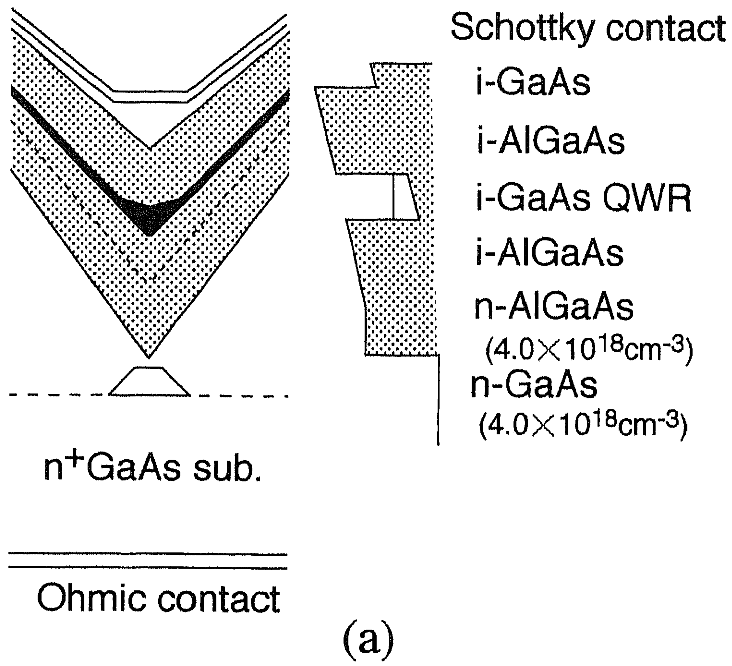

(a)

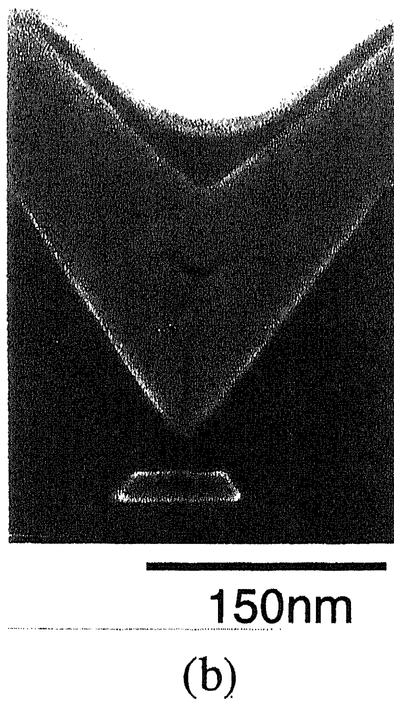

(b)

Fig. 5.1 Schematic illustrations and a scanning electron microscope image of the sample used in the experiments.

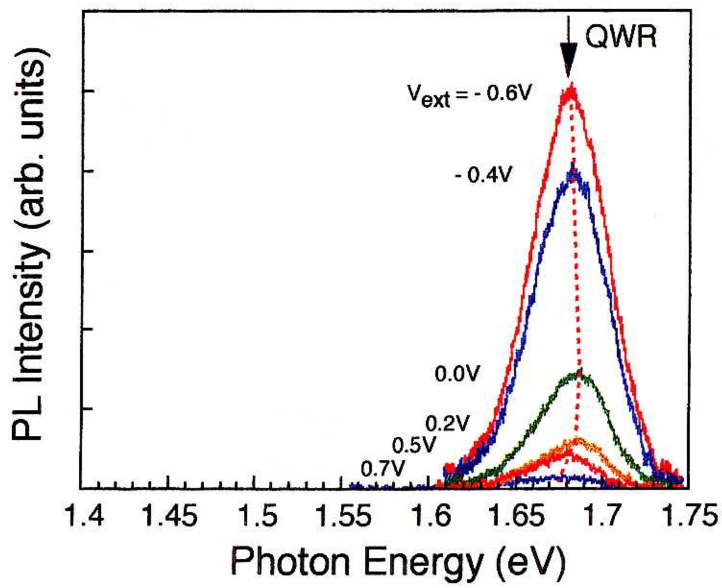

(a)

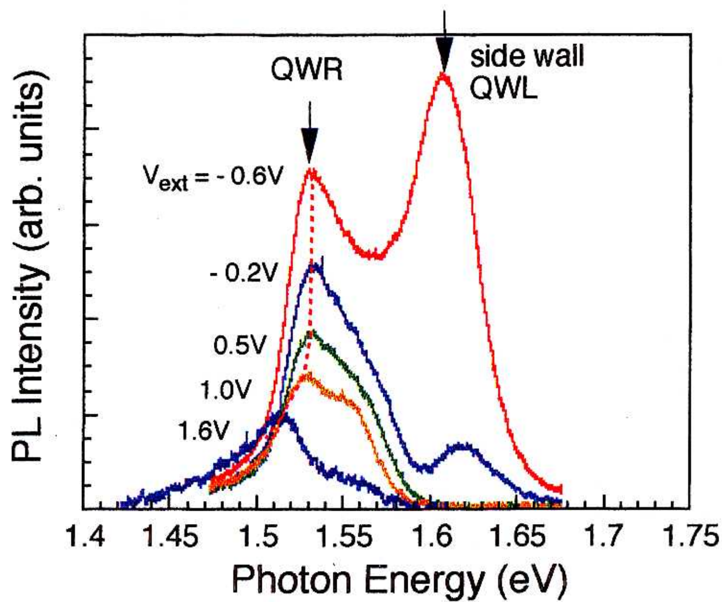

(b)

Fig. 5.2 Dependence of PL spectra on the externally applied voltage Vext in the case of lateral width of the quantum wire Lx = 8nm (a), Lx = 35 nm (b) .

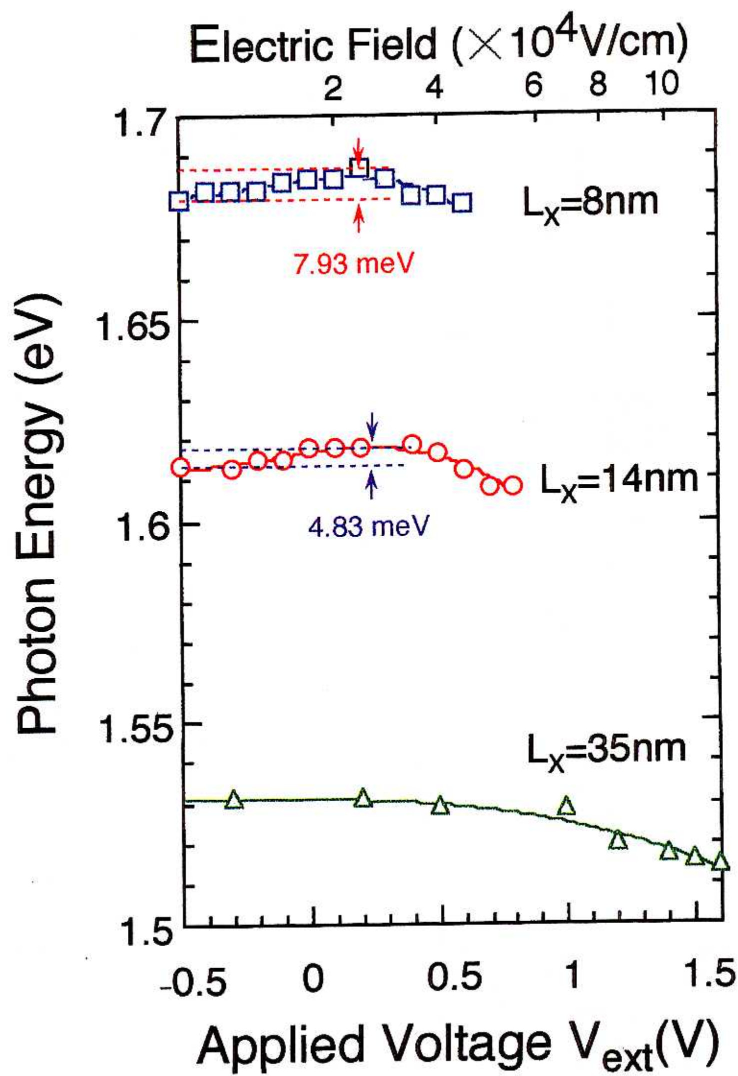

Fig. 5.3 PL peak positions of the quantum wires of various dimensions as a function of the externally applied voltage (electric field).

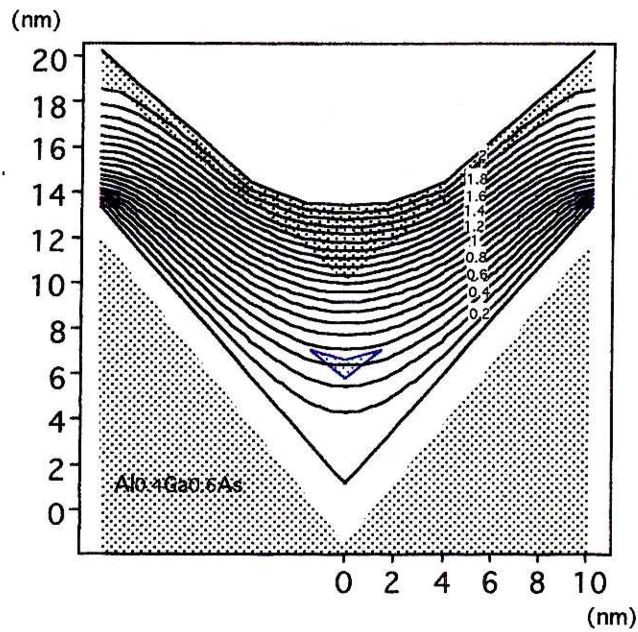

(a)

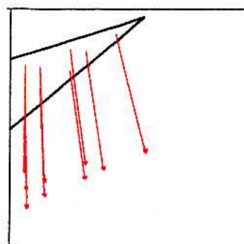

(b)

Fig. 5.4 (a) Distribution of an electric field in the QWR structure calculated with the finit element method (applied voltage is 2.0 V). (b) Direciton of the electric field in the QWR.

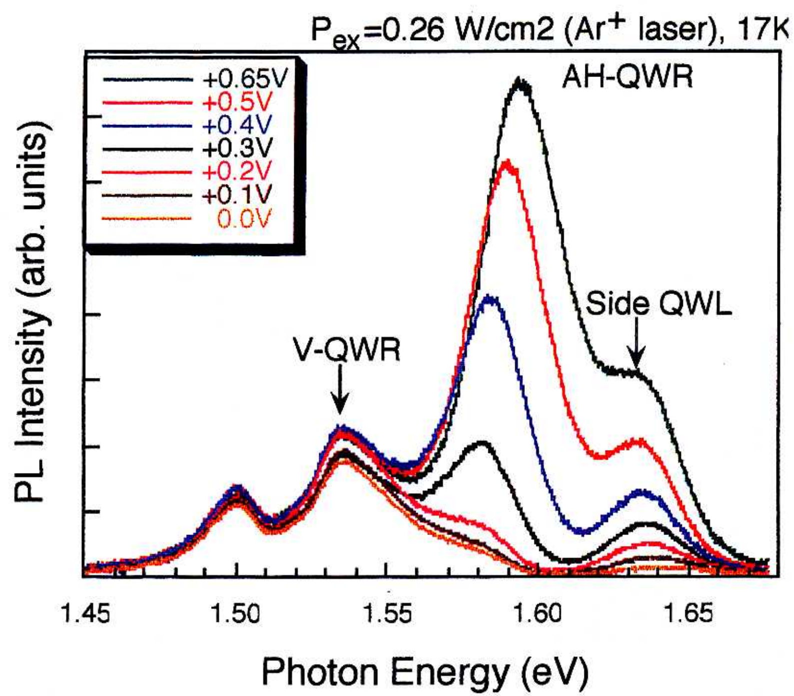

Fig. 5.5 PL spectra for the sample with arrow-head shaped QWRs (AH-QWRs) which are formed on top of the triangula prisms.

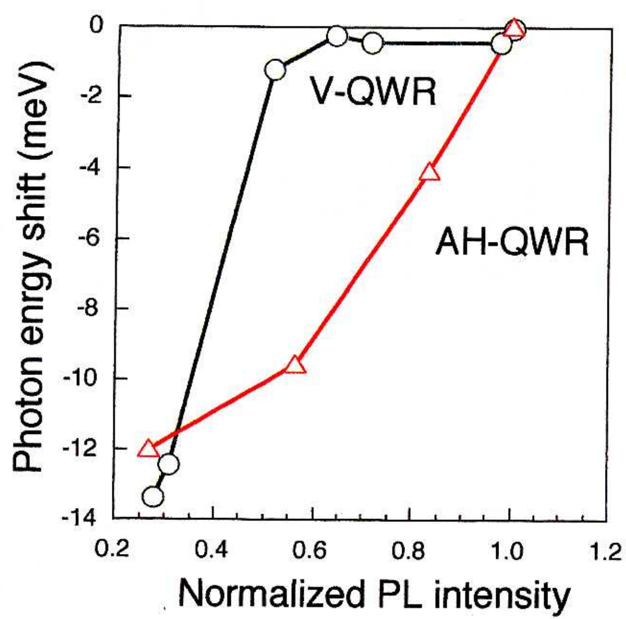

Fig. 5.6 Dependence of PL intensity on the energy shift witl respect to V-shaped (V-QWR) and arrow-head (AH-QWI quantum wires.

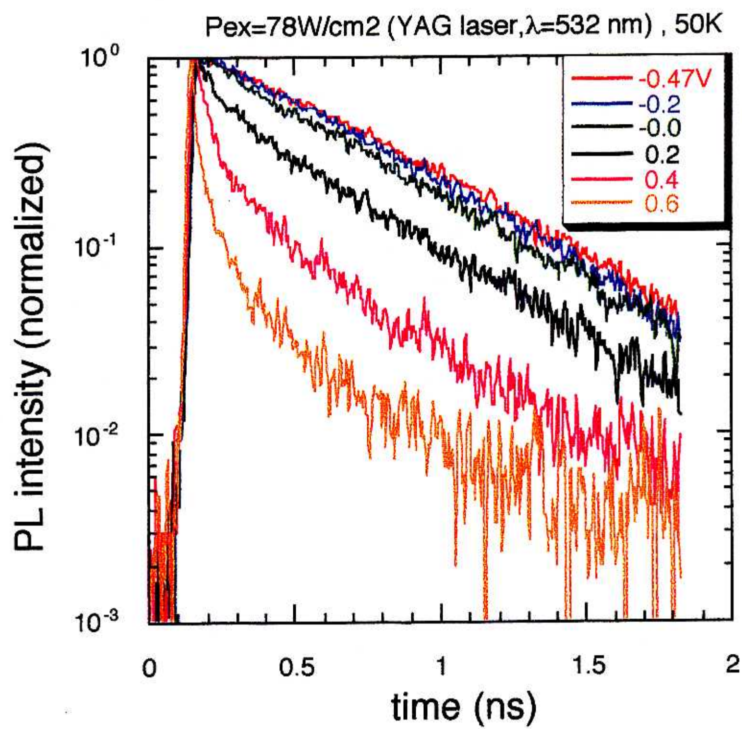

Fig. 5.7 Temporal evolution of the PL peaks associated with the quantum wire transition (Lx=8 nm) at various Vext. The data were normalized at their maximal.

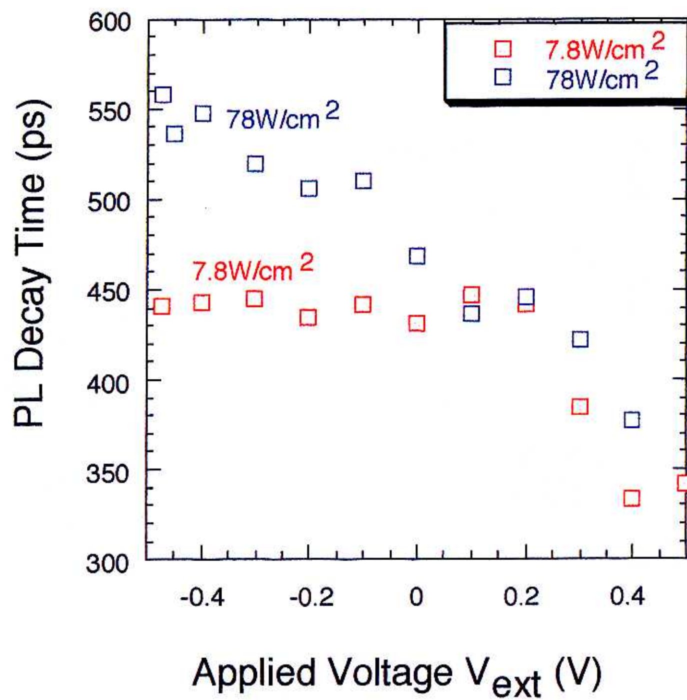

Fig.5.8 PL decay times were plotted as a function of applie(voltage at two kinds of excitation powers (P_{ex}=7.8 W/cm^2, 78 W/cm^2).

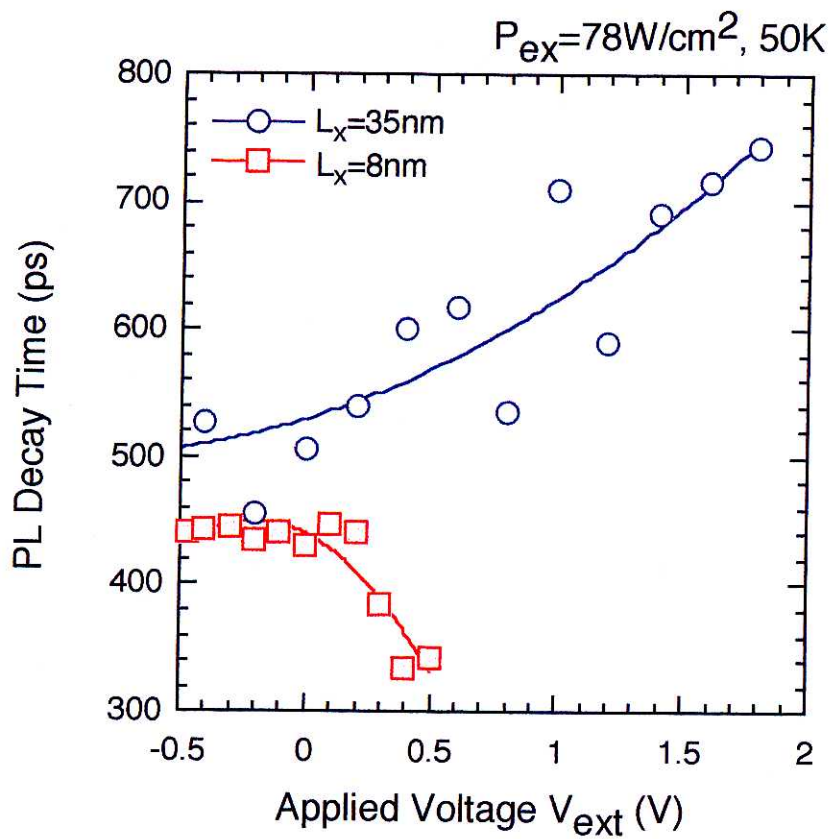

Fig. 5.9 The dependence of PL decay time on the Vext and L_x.

Chapter 6

Conclusion

In this thesis, optical properties of GaAs and InGaAs QWR structures and a new method of fabrication of QWR structures, as a basic study for application of QWRs to actual devices, were investigated. In addition, QWR laser structures with a microcavity and the quantum confined Stark effect in QWRs were demonstrated in order to show the feasibility of the QWRs for application to optical devices.

In Chapter 2, the fabrication technique of GaAs and InGaAs quantum wires using the selective MOCVD was reviewed. The optical properties of the QWRs are also discussed by using photoluminescence (PL) measurements, photoluminescence excitation (PLE) measurements, measurements with near-field scanning optical microscope (NSOM), and cathodoluminescence measurements (CL). Temperature dependence of the FWHMs demonstrated that the broadening of emission peak of the QWRs are suppressed at higher temperature, which probably reflects the density of states in QWRs. From the temperature dependence of PL intensity, the QWR structures are promising for applications to optical devices such as laser diodes and optical switching devices operated in room temperature. PLE results exhibited clear peaks corresponding to the quantized transition levels and the anisotropic polarization dependence. The subband spacings for the GaAs QWRs was rather large (50 meV) and the

spacing was enhanced by introducing strained InGaAs QWRs. NSOM measurements at room temperature demonstrated the sharp lines from the QWRs. The origins of the PL peaks were identified with CL measurements.

In Chapter 3, we discussed the fabrication of ridge-type InGaAs QWR structures on a (110) cleaved plane of AlGaAs/GaAs superlattice by using selective growth. Spatially resolved PL of the QWRs were observed for the first time by using μ-PL measurements at low temperature, showing their polarization dependence. We also observed spatial μ-PL images of carrier diffusion in the InGaAs QWRs, showing anisotropic PL distribution along the wire. The FWHM of PL peak of the QWRs was a little broad compared with the V-shaped QWRs in spite of good uniformity of mask patterns. Growth condition needs more optimization in order to better quality of QWRs.

In Chapter 4, a vertical microcavity InGaAs strained QWR lasers were investigated using MOCVD selective growth as a step toward the ultimate lasers.

Fabrication process of the 4λ- and 2λ-cavity laser structures were discussed and the problems in fabrication were revealed. In particular, flattening the spacer layer above the QWRs are important.

With respect to the 4λ-cavity lasers, optical characteristics were investigated. The cavity effect was evidenced by the difference of the PL broadening with and without the cavity. Lasing was observed at 77K by using optical pumping. The threshold input power was very low and the feasibility of the QWRs for laser diodes was demonstrated.

The lasing oscillation was also confirmed by time resolved measurements.

In Chapter 5, the QCSE in the GaAs quantum wires was experimentally investigated. We demonstrated the observation of a blue shift of the PL peak in the GaAs quantum wires with various sizes. We believe this blue shift results from the enhanced excitonic effect due to the strong confinement in the nanostructures. The blue shift results in large absorption change with small change of wavelength. This feature is suitable for optical modulators. Therefore, the QWR structure is very promising for them. In order to increase the total change of absorptions, higher density of QWRs requires, for example, by stacking the QWRs. Time resolved PL measurements were also performed. As a result, we found the recombination lifetime of the exciton emission line depends strongly on the dimension of the quantum wire. That is, the PL decay time decreased in small quantum wires with the increase of electric fields, while it increased in large quantum wires. This results shows that when the quantum wire is narrower, tunneling mechanism of carriers dominates reduction of overlap of the wavefunction of electrons and holes.

In this work, optical properties of GaAs and InGaAs QWRs are revealed. A new method of fabrication of QWR structures was proposed, as a fundamental study for application of QWRs to actual devices. Furthermore, feasibility of optical devices based on the QWR structures was successfully demonstrated. The author hopes that the

present study contributes to the fundamental understanding of the quantum wire and applications to the optical devices.

Bibliography

[1] H. Sakaki, "Scattering suppression and high-mobility effect of size-quantized electrons in ultrafine semiconductor wire structures", Jpn. J. Appl. Phys. **19**, L735 (1980).

[2] D. A. B. Miller, D. S. Chemla, and S. Schmitt-Rink, "Electroabsorption of highly confined systems: Theory of the quantum-confined Franz-Keldysh effect in semiconductor quantum wires and dots", Appl. Phys. Lett. **52**, 2154 (1988).

[3] S. Schmitt-Rink, D. A. B. Miller, and D. S. Chemla, "Theory of the linear and nonlinear optical properties of semiconductor microcrystallites", Phys. Rev. B 8113 (1987).

[4] T. Arakawa, M. Nishioka, Y. Nagamune, and Y. Arakawa, "Fabrication of vertical-microcavity quantum wire lasers", Appl. Phys. Lett. **64**, 2200 (1994).

[5] Y. Arakawa, and H. Sakaki, "Multidimensional quantum well laser and temperature dependence of its threshold current", Appl. Phys. Lett. **40**, 939 (1982).

[6] K. Kash, A. Scherer, J. M. Worlock, H. G. Craighead, and M. C. Tamargo, "Optical spectroscopy o fultrasmall structures etched from quantum wells", Appl. Phys. Lett. **49**, 1043 (1986).

[7] J. Cibert, P. M. Petroff, G. J. Dolan, S. J. Pearton, A. C. Grossard, and J. H. English, "Optically detected carrier confinement to one and zero dimension in GaAs quantum well wires and boxes", Appl. Phys. Lett. **49**, 1275 (1986).

[8] H. Temkin, G. L. Dolan, M. B. Panish, and S. N. G. Chu, "Low-temperature photouminescence from InGaAs/InP quantum wires and boxes", Appl. Phys. Lett. **50**, 413 (1987).

[9] D. Gershoni, H. Temin, G. L. Dolan, J. Dunsmuir, S. N. G. Chu, and M. B. Panish, "Effects of two-dimensional confinement on the optical properties of InGaAs/InP quantum wire structures", Appl. Phys. Lett. **53**, 995 (1988).

[10] B. I. Miller, A. Shahar, U. Koren, and P. J. Corvini, "Quantum wires in InGaAs/InP fabaricated by holographic photolithography", Appl. Phys. Lett. **54**, 188 (1989).

[11] M. Notomi, M. Naganuma, T. Nishida, T.Tamamura, H. Iwamura, S. Nojima, and M. Okamoto, "Clear energy level shift in ultranarrow InGaAs/InP quantum well wires fabricated by reverse mesa chemical etching", Appl. Phys. Lett. **58**, 720 (1991).

[12] P. M. Petroff, A. C. Gossard, and W. Wiegmann, "Structure of AlAs-GaAs interfaces grown on (100) vicinal surfaces by molecular beam epitaxy", Appl. Phys. Lett. **45**, 621 (1984).

[13] J. M. Gaines, P. M. Petroff, H. Kroemer, R. J. Simes, R. S. Geels, and J. H. English, "Molecular-beam epitaxy growth of tilted GaAs/AlAs superlattices by deposition of fractional monolayers on vicinal (001) substrates", J. Vac. Sci. Technol. **B6**, 1378 (1988).

[14] M. Tsuchiya, P. M. Petroff, and L. A. Colden, "Spontaneous growth of coherent tilted superlattice on vicinal (100) GaAs substrates", Appl. Phys. Lett. **54**, 1690 (1989).

[15] T. Fukui, and H. Saito, "(AlAs)1/2(GaAs)1/2 fractional-layer superlattices grown on (001) vicinal GaAs substrates by metal-organic chemical vapor deposition", J. Vac. Sci. Technol. **B6**, 1373 (1988).

[16] S. Hasegawa, M. Sato, K. Maehashi, H. Asahi, and H. Nakashima, "Formation of quantum well wire-like structures by MBE growth of AlGaAs/GaAs superlattices on GaAs (110) surfaces", J. Cryst. Growth **111**, 371 (1991).

[17] R. Bhat, E. Kapon, D. M. Hwang, M. A. Koza, and C. P. Yun, "Patterned quantum well heterostructures grown by OMCVD on non-planar substrates: applications to extremely narrow SQW lasers", J. Cryst. Growth **93**, 850 (1988).

[18] T. F. a. S. Ando, "New GaAs Quantum Wires on (111) B facets by Selective MOCVD", Electron. Lett. **25**, 410 (1989).

[19] J. A. Lebens, C. S. Tsai, and K. J. Vahala, "Application of selective epitaxy to fabarication of nanometer scale wire and dot structures", Appl. Phys. Lett. **56**, 2642 (1990).

[20] T. Fukui, S. Ando, and Y. K. Fukai, "Lateral quantum well wires fabricated by selective metalorganic chemical vapor deposition", Appl. Phys. Lett. **57**, 1209 (1990).

[21] T. F. Kuech, M. S. Goorsky, M. A. Tischler, A. Palevski, P. Solomon, R. Potemski, C. S. Tsai, J. A. Lebens, and K. J. Vahala, "Selective epitaxy of GaAs, AlxGa1-xAs, and InxGa1-xAs", J. Cryst. Growth **107**, 116 (1991).

[22] C. S. Tsai, J. A. Lebens, C. C. Ahn, A. Nouhi, and K. J. Vahala, "Facet modulation selective exitaxy--a technique for quantum well wire doublet fabrication", Appl. Phys. Lett. **60**, 240 (1992).

[23] T. Fukui, and S. Ando, "New GaAs Quantum Wires on {111}B facets by selective MOCVD", Electron. Lett. **25**, 410 (1989).

[24] S. Ando, and T. Fukui, "Facet growth of AlGaAs on GaAs with SiO_2 gratings by MOCVD and applications to quantum well wires", J. Cryst. Growth **98**, 646 (1989).

[25] S. Tsukamoto, Y. Nagamune, M. NIshioka, and Y. Arakawa, "Fabrication of GaAs quantum wires on epitaxially grown V grooves by metal-organic chemical-vapor deposition", J. Appl. Phys. **71**, 533 (1992).

[26] L. Pfeiffer, K. W. West, H. L. Stormer, J. P. Eisenstein, K. W. Baldwin, D. Gershoni, and J. Spector, "Formation of a high quality two-dimensional electron gas on cleaved GaAs", Appl. Phys. Lett. **56**, 1697 (1990).

[27] Y. C. Chang, L. L. Chang, and L. Esaki, "A new one-dimensional quantum well structure", Appl. Phys. Lett. **47**, 1324 (1985).

[28] W. Wegscheider, L. N. Pfeiffer, M. M. Dignam, K. West, S. L. McCall, and R. Hull, "Lasing from Excitons in Quantum Wires", Phys. Rev. Lett. **71**, 4071 (1993).

[29] T. Someya, H. Akiyama, and H. Sakaki, "Laterally squeezed excitonic wave function in quantum wires", Phys. Rev. Lett. **74**, 3664 (1995).

[30] M. Notomi, Y. Kadota, and T. Tamamura, "Novel Selective Growth Using a Native Oxide on a (110) Cleaved Plane of AlGaAs/GaAs Superlattice", Jpn. J. Appl. Phys **34**, 1451 (1995).

[31] M. Cao, P. Daste, Y. Miyamoto, Y. Miyake, S. Nogiwa, S. Arai, K. Furuya, and Y. Suematsu, "GaInAsP/InP single-quantum-well (SQW) laser with wire-like active region towards quantum wire laser", Electron. Lett. **24**, 824 (1988).

[32] E. Kapon, S. Simhony, R. Bhat, and D. M. Hwang, "Single quantum wire semiconductor lasers", Appl. Phys. Lett. **55**, 2715 (1989).

[33] M. Walther, E. Kapon, C. Caneau, D. M. Hwang, and L. M. Schiavone, "InGaAs/GaAs strained quantum wire lasers grown by organometallic chemical vapor deposition on nonplanar substrates", Appl. Phys. Lett. **62**, 2170 (1993).

[34] Y. Miyake, H. Hirayama, S. Arai, Y. Miyamoto, and Y. Suematsu, "Room temperature operation of GaInAs-GaInAsP-InP SCH multiquantum-film laser with narrow wire-like active region", IEEE Photonics Technol. Lett. **3**, 191 (1991).

[35] H. Saito, K. Uwai, and N. Kobayashi, "GaAs quantum-wire laser using fractional layer superlattice", Jpn. J. Appl. Phys. **32**, 4440 (1993).

[36] J. Yoshida, and K. Kishino, "Low threshold current density operation of GaInP-AlGaInP visible multiple quantum wire-like lasers (MQWR-LDs) under the room temperature pulsed condition", IEEE Photonics Technol. Lett. **7**, 241 (1995).

[37] W. Wegscheider, A. L. Pfeiffer, K. West, and R. E. Leibenguth, "Current injection GaAs/AlGaAs quantum wire lasers fabricated by cleaved edge overgrowth", Appl. Phys. Lett. **65**, 2510 (1994).

[38] N. D. Jong Chang Yi L. A. Coldren, "Investigation of tilted superlattices for quantum-wire laser applications", Appl. Phys. Lett. **59**, 3015 (1991).

[39] Y. Arakawa, K. Vahala, and A. Yariv, "Quantum noise and dynamics in quantum well and quantum wire lasers", Appl. Phys. Lett. **45**, 950 (1984).

[40] Y. Nagamune, S. Tsukamoto, M. Nishioka, and Y. Arakawa, "Fabrication of InGaAs strained quantum wires using selective MOCVD growth on SiO_2-patterned GaAs substrate", J. Cryst. Growth **126**, 707 (1993).

[41] Y. Yamauchi, T. Takahashi, J. N. Shulman, and Y. Arakawa, "Quantum wires with strain effect: Tight-binding analysis", Surf. Sci. **267**, 291 (1992).

[42] T. Yamauchi, T. Takahash, J. Schulman, and Y. Arakawa, "Theoretical analysis of band structures and lasing characteristics in strained quantum wire lasers", IEEE J. Quantum Electron. **29**, 2109 (1993).

[43] S. Ueno, Y. Miyake, and M. Asada, "Advantage of strained quantum wire lasers", Jpn. J. Appl. Phys. **31**, 286 (1992).

[44] Y. Arakawa, and A. Yariv, "Quantum well lasers-gain, spectra, dynamics", IEEE J. Quantum Electron. **22**, 1887 (1986).

[45] M. Nishioka, S. Tsukamoto, Y. Nagamune, T. Tanaka, and Y. Arakawa, "Fabrication of InGaAs strained quantum wires using selective MOCVD growth on SiO_2-patterned GaAs substrate", J. Cryst. Growth **124**, 502 (1992).

[46] J. Christen, M. Grundmann, E. Kapon, E. Colas, D. M. Hwang, and D. Bimberg., "Ultrafast carrier capture and long recombination lifetimes in GaAs quantum wires grown on nonplanar substrates", Appl. Phys. Lett. **61**, 67 (1992).

[47] A. Gustafsson, F. Reinhardt, G. Biasiol, and E. Kapon, "Low-pressure organometallic chemical vapor deposition of quantum wires on V-grooved substrates", Appl. Phys. Lett. **67**, 3673 (1995).

[48] S. Tsukamoto, Y. Nagamune, M. Nishioka, and Y. Arakawa, "Fabrication of GaAs arrowhead-shaped quantum wires by metalorganic chemical vapor deposition selective growth", Appl. Phys. Lett. **62**, 49 (1993).

[49] S. Tsukamoto, Y. Nagamune, M. Nishioka, and Y. Arakawa, "Fabrication of GaAs quantum wires (~10 nm) by metalorganic chemical vapor selective deposition growth", Appl. Phys. Lett. **63**, 355 (1993).

[50] E. Kapon, M. C. Tamargo, and D. M. Hwang, "Molecular beam epitaxy of GaAs/AlGaAs superlattice heterostructures on nonplanar substrates", Appl. Phys. Lett. **50**, 347 (1987).

[51] R. Rinaldi, and M. Ferrara, "Evidence of one-dimensional excitons in GaAs V-shaped quantum wires", Phys. Rev. B **50**, 11795 (1994).

[52] X. L. Wang, M. Ogura, and H. Matushata, "Temperature dependent photoluminescence investigation of AlGaAs/GaAs

quantum wires grown by flow rate modulation epitaxy", Appl. Phys. Lett. **67**, 3629 (1995).

[53] X. L. Wang, M. Ogura, and H. Matsuhata, "Carrier capture efficiency of AlGaAs/GaAs quantum wires affected by composition nonuniformity of an AlGaAs barrier layer", Appl. Phys. Lett. **67**, 804 (1995).

[54] T. Tanaka, T. Yamauchi, and Y. Arakawa, , Proc. 52th Autumn Meeting of the Japan Society of Applied Physics, Okayama (1991).

[55] D. S. Citrin, and Y. C. Chang, "Subband structures of semiconductor quantum wires from the effective bond-orbital model", J. Appl. Phys. **68**, 161 (1990).

[56] L. B. Freund, and T. J. Gosling, "Critical thickness condition for growth of strained quantum wires in substrate V-grooves", Appl. Phys. Lett. **66**, 2822 (1995).

[57] R. Rinaldi, R. Cingolani, L. DeCaro, M. Lomascolo, M. DiDio, L. Tapfer, U. Marti, and F. K. Reinhart, "Optical spectroscopy of InGaAs/GaAs V-shaped quantum wires", J. Opt. Soc. Am. B. **13**, 1031 (1996).

[58] G. Vermeire, Z. Q. Yu, F. Vermaerke, L. Buydens, P. V. Daele, and P. Demeester, "Anisotropic photoluminescence behaviour of vertical AlGaAs structures grown on gratings", J. Cryst. Growth **124**, 513 (1992).

[59] D. Moroni, J. P. Andre, E. P. Menu, P. Gentric, and J. N. Paatillon, "Photoluminescence investigation of InGaAs-InP quantum wells", J. Appl. Phys. **62**, 2003 (1987).

[60] E. Kapon, D. M. Hwang, and R. Bhat, "Stimulated Emission in Semiconductor Quantum Wire Heterostructures", Physical Review Letters **63**, 430 (1989).

[61] E. Kapon, G. Biasiol, D. M. Hwang, E. Colas, and M. Walther, "Self-Ordering Mechanism of Quantum Wires Grown on Nonplanar Substrate", Solid State Electronics **40**, 815 (1996).

[62] R. D. Grober, T. D. Harris, J. K. Trautman, E. Betzig, W. Wegsheider, L. Pfeiffer, and K. West, "Optical spectroscopy of a GaAs/AlGaAs quantum wire structure using near-field scanning optical microscopy", Appl. Phys. Lett. **64**, 1421 (1994).

[63] Y. Toda, M.Kourogi, M. Ohtsu, Y. Nagamune, and Y. Arakawa, "Spatially and spectrally resolved imaging of GaAs quatum-dot structures using near-field optical technique", App. Phys. Lett. **69**, 827 (1996).

[64] E. Betzig, and J. K. Trautman, , Science **257**, 189 (1992).

[65] S. H. Jones, and K. M. Lau, "Selective area growth of high quality GaAs by OMCVD using native oxide masks", J. Electrochem. Soc. **134**, 3149 (1987).

[66] Y. Hiratani, Y. Ohki, Y. Sugimoto, K. Akita, M. Taneya, and H. Hidaka, "Selective area epitaxy of GaAs using GaAs oxide as a mask", Jpn. J. Appl. Phys. **29**, L1360 (1990).

[67] A. R. Sugg, J. N. Holonyak, J. E. Baker, F. A. Kish, and J. M. Dallessasse, "Native oxide stabilization of AlAs-GaAs heterostructures", Appl. Phys. Lett. **58**, 1199 (1991).

[68] R. S. Burton, T. E. Schlesinger, D. J. Holmgren, S. C. Smith, and R. D. Burnham, "Self-aligned native-oxide ridge-geometry $Al_xGa_{1-x}As$-GaAs quantum well heterostructure laser arrays", Appl. Phys. Lett. **60**, 1776 (1992).

[69] K. Okamoto, M. Furuta, and K. Yamaguchi, "Lateral growth on (110) GaAs substrates by metalorganic chemical vapor deposition", Jpn. J. Appl. Phys. **27**, L437 (1988).

[70] R. P. Gale, R. W. McClelland, J. C. C. Fan, and C. O. Bozler, "Lateral epitaxial overgrowth of GaAs by organometallic chemical vapor deposition", Appl. Phys. Lett. **41**, 545 (1982).

[71] H. Akiyama, T. Someya, and H. Sakaki, "Optical anisotropy in 5-nm-scale T-shaped quantum wires fabricated by the cleaved-edge overgrowth method", Physical Review B **53**, 4229 (1996).

[72] Y. Nagamune, H. Watabe, F. Sogawa, and Y. Arakawa, "One-dimensional exciton diffusion in GaAs quantum wires", Appl. Phys. Lett. **67**, 1535 (1995).

[73] Y. Nagamune, Y. Arakawa, S. Tsukamoto, M. Nishioka, S. Sakaki, and N. Miura, "Photoluminescence spectra and anisotropic energy shift of GaAs quantum wires in high magnetic fields", Phys. Rev. Lett. **69**, 2963 (1992).

[74] F. Koyama, S. Kinoshita, and K. Iga, "Room-temperature continuous wave lasing characteristics of a GaAs vertical cavity surface-emitting laser", Appl. Phys. Lett. **55**, 221 (1989).

[75] J. L. Jewel, A. Scherer, S. L. McCall, Y. H. Lee, S. J. Walker, J. P. Harbison, and L. T. Florez, "Low-threshold electrically pumped vertical-cavity surface-emitting microlasers", Electron. Lett. **25**, 1123 (1989).

[76] E. Yablonovitch, T. J. G. Gmitter, and R. Bath, "Inhibited and enhanced spontaneous emission from optically thin AlGaAs/GaAs double heterostructures", Phys. Rev. Lett. **61**, 2546 (1988).

[77] T. Baba, T. Hamano, F. Koyama, and K. Iga, "Spontaneous Emission Factor of a Microcavity DBR Surface-Emitting Laser", IEEE J. Quantum Electron. **27**, 1347 (1991).

[78] C. Weisbuch, A. Ishikawa, M. Nishioka, and Y. Arakawa, "Observation of the coupled exciton-photon mode splitting in a semiconductor quantum microcavity", Phys. Rev. Lett. **69**, 3314 (1992).

[79] Y. Arakawa, "Quantum wire and box lasers", Extended Abstracts of the 1990 Int. Conf. on Solid State Devices and Materials (The Japan Society of Applied Physics, Sendai). 745 (1990).

[80] A. Chavez-Pirson, H. Ando, H. Saito, and H. Kanbe, "Quantum wire microcavity laser made from GaAs fractinal layer superlattices", Appl. Phys. Lett. **64**, 1759 (1994).

[81] Y. M. S. Ueno Y. Suematsu, "Advantage of strained quantum wire lasers", Jpn. J. Appl. Phys. **31**, 286 (1992).

[82] T. Mukai, T. Kawakami, T. Yoshikawa, and M. Sugimoto, "Record Low Threshold Current in Microcavity Surface-Emitting Laser", Jpn. J. Appl. Phys. **32**, L1533 (1993).

[83] F. Sogawa, "Ultrafast Dynamids in Microcavity Optical Devices", Doctor thesis (1997).

[84] T. H. Wood, C. A. Burrus, D. A. B. Miller, D. S. Chemla, T. C. Damen, A. C. Gossard, and W. Wiegmann, "High-speed optical modulation with GaAs/GaAlAs quantum wells in a p-i-n diode structure", Appl. Phys. Lett. **44**, 16 (1984).

[85] D. A. B. Miller, D. S. Chemla, T. C. Damen, A. C. Gossard, W. Wiegmann, T. H. Wood, and C. A. Burrus, "Band-edge electroabsorption in quantum well structures: the quantum-confined Stark effect", Phys. Rev. Lett. **53**, 2173 (1984).

[86] G. Bastard, E. E. Mendez, L. L. Chang, and L. Esaki, "Variational calculations on a quantum well in an electric field", Phys. Rev. B **28**, 3241 (1983).

[87] D. A. B. Miller, D. S. Chemla, T. C. Damen, A. C. Gossard, W. Wiegmann, T. H. Wood, and J. C. A. Burrus, "Novel Hybrid Optically Bistable Switch: The Quantum Well Self-Electro-Optic Effect Device", Appl. Phys. Lett. **45**, 13 (1984).

[88] O. Schilling, A. Forchel, A. Kohl, and Brittner, "Optical analysis of quantum confined Stark effect in overgrown InGaAs/InP quantum wires", J. Vac. Sci. Technol. B **11**, 2556 (1993).

[89] S. Benner, and H. Haug, "Influence of external electric and magnetic fields on the excitonic absorption spectra of quantum-well wires", Phys. Rev. B **47**, 15750 (1993).

[90] T. Arakawa, Y. Kato, F. Sogawa, and Y. Arakawa, "Quantum Confined Stark Effects in Quanum Wires and Dots", Collected Abstracts of International Symposium on Formation, Physics and Device Application of Quantum Dots Structures (QDS) 184 (1996).

[91] K. W. Goossen, E. A. Caridi, T. Y. Chang, J. B. Stark, D. A. B. Miller, and R. A. Morgan, "Observation of room-temperature blue shift and bistability in a strained InGaAs-GaAs <111> self-electro-optic effect device", Appl. Phys. Lett. **56**, 715 (1990).

[92] S. Marcinkevicius, U. Olin, M. Ottossson, G. Treideris, I. Simkiene, and T. Lideikis, "Stark shift of the interband transitions in asymmetric step InGaAs/GaAs quantum wells", J. Appl. Phys. **73**, 4691 (1993).

[93] A. S. Pabla, J. L. Sanchez-Rojas, J. Woodhead, R. Grey, J. P. R. David, G. J. Rees, R. A. Hogg, T. A. Fisher, A. R. K. Willcox, D. M. Whittaker, M. S. Skolnick, and D. J. Mowbray, "Tailoring of internal fields in InGaAs/GaAs multiwell structures grown on (111)B GaAs", Appl. Phys. Lett. **63**, 752 (1993).

[94] H. J. Polland, L. Schultheis, J. Kuhl, E. O. Gobel, and C. W. Tu, "Lifetime Enhancement of Two-Dimensional Excitons by the Quantum-Confined Stark Effect", Phys. Rev. Lett. **55**, 2610 (1985).

[95] E. H. Austin, and M. Jaros, "Electric field induced shifts and lifetimes in GaAs-GaAlAs quantum wells", Appl. Phys. Lett. **47**, 274 (1985).

Publication List

1 Technical Journals

1) T. Arakawa, S. Tsukamoto, M. Nishioka, Y. Nagamune, J. Lee and Y. Arakawa," Fabrication of InGaAs Strained Quantum Wire Structures Using Selective-Area Metal-Organic Chemical Vapor Deposition Growth.", Jpn. J. Appl. Phys. **32**, L1377(1993).

2) T. Arakawa, M. Nishioka, Y. Nagamune,and Y. Arakawa, "Fabrication of Vertical-Microavity Quantum-Wire Lasers", Appl. Phys. Lett. **64**, 2200 (1994).

3) T. Arakawa, H. Watabe, H. Hayashi, and Y. Arakawa, "Fabrication and micro-photoluminescence imaging of ridge-type InGaAs quantum wires grown on a (110) plane of AlGaAs/GaAs superlattice", Appl. Phys. Lett. **69**, 1294 (1996).

4) T. Arakawa, Y. Kato, F. Sogawa, and Y. Arakawa, "Photoluminescence Studies of GaAs Quantum Wires with Quantum Confined Stark Effect", Appl. Phys. Lett. **70**, 646 (1997).

2 International Conferences

1) S. Tsukamoto, Y. Nagamune, M. Nishioka, T. Arakawa, and Y. Arakawa, "Fabrication of Thin GaAs Quantum Wires(~10nm) by MOCVD Growth", The International Symposium on Gallium Arsenide and Related Compounds, Karuizawa, Sep. 28- Oct.2, 1992.

2) T. Arakawa, S. Tsukamoto, M. Nishioka, Y. Nagamune, J. Lee and Y. Arakawa," Fabrication of InGaAs Strained Quantum Wires Using MOCVD Selective Growth and their Optical Properties", The 1993 Inernational Conference on Solid State Device and Materials , Makuhari, Aug.29-Sep.1,1993.

3) T. Arakawa, S. Tsukamoto, Y. Nagamune, M. Nishioka, J. Lee and Y. Arakawa, "InGaAs Strained Quantum Wire Laser Structures Fabricated by Selective-Area MOCVD Growth",1993 International Semiconductor Device Research Symposium, Charlottesville, Dec. 1-3, 1993.

4) T. Arakawa,T. Kono, M. Nishioka, Y. Nagamune,and Y. Arakawa, "Fabrication of Strained Quantum Wire Laser Structure with Vertical Microcavity", The14th Microoptics Conference and the 11th Topical Meeting on Gradient-Index Optical Systems (MOC/GRIN) '93, Kawasaki, Oct. 20-22, 1993.

5) T. Arakawa, M. Nishioka, Y. Nagamune, and Y. Arakawa, "Strained quantum wire laser with a vertical microcavity", Conference on lasers and electro-optics (CLEO), Anaheim, USA, 1994.

6) T. Arakawa, H. Wabate, H. Hayashi, and Y. Arakawa, "Fabrication and micro-photoluminescence imaging of ridge-type InGaAs quantum wires grown on a (110) plane of AlGaAs/GaAs superlattice", Quantum Electronics and Laser Science Conference, QThC6, Anaheim, June 2-7, 1996.

7) T. Arakawa, Y. Kato, F. Sogawa, and Y. Arakawa, "Quantum Confined Stark Effects in Quanum Wires and Dots, International Symposium on Formation, Physics and Device Application of Quantum Dots Structures (QDS '96), Th2-5, Hokkaido University Conference Hall, Sapporo, Japan, November 4-7, 1996.

3 Domestic Conferences (presented in Japanese) Related to This Thesis

1)T. Tsukamoto, Y. Nagamune, M. Nishioka, T. Arakawa, T. Kono, and Y. Arakawa, "Fabrication of GaAs Quantum Wires by

MOCVD Selective Growth and their Optical Properties", The 10th Symposium on Semiconductor Lasers, Kanagawa, March 1993.

2) S. Tsukamoto, Y. Nagamune, T. Arakawa, M. Nishioka, and Y. Arakawa, "Fabrication of GaAs Quantum Wire Structures (~10 nm) and their Optical Properties", The 40th Spring Meeting, 1993; The Japan Society of Applied Physics and Related Societies, Tokyo, March 1993.

3) T. Arakawa, S. Tsukamoto, M. Nishioka, Y. Nagamune, and Y. Arakawa, "Fabrication of InGaAs Strained Quantum Wires using Selective MOCVD Growth and their Optical Properties", The 40th Spring Meeting, 1995; The Japan Society of Applied Physics and Related Societies, Tokyo, March 1993.

4) T. Arakawa, S. Tsukamoto, M. Nishioka, Y. Nagamune, J. Lee and Y. Arakawa," Fabrication of InGaAs Strained Quantum Wires Using MOCVD Selective Growth and their Optical Properties", 12th Symposium on Alloy Semiconductor Physics and Electronics, Shizuoka, July 14-16,1993.

5) T. Arakawa, M. Nishioka, S. Tsukamoto, Y. Nagamune, and Y. Arakawa, "Fabrication of InGaAs Strained Quantum Wire Laser by Selective Area MOCVD Growth", The 54th Autumn Meeting, 1993; The Japan Society of Applied Physics, Hokkaido, September 1994.

6) T. Arakawa, M. Nishioka, Y. Nagamune, and Y. Arakawa, "Fabrication of Vertical-Cavity Strained Quanum Wire Lasers by Selective MOCVD Growth", The 41st Spring Meeting, 1995; The Japan Society of Applied Physics and Related Societies,, Tokyo, March 1994.

7) T. Arakawa, H. Watabe, M. Nishioka, and Y. Arakawa, "Fabrication of InGaAs Quantum Wires on Cleaved Edge of

GaAs/AlGaAs Superlattice", The 56h Autumn Meeting, 1995; The Japan Society of Applied Physics, Kanazawa, Octobor 1995.

8) T. Arakawa, T. Tanaka, M. Nishioka, and Y. Arakawa, "Quantum Confined Stark Effect in GaAs Quantum Wires", The 43rd Spring Meeting, 1996; The Japan Society of Applied Physics and Related Societies, Saitama, March 1996.

9) Y. Toda, S. Shinomori, T. Arakawa, M. Kitamura, Y. Nagamune, Y. Arakawa, and M. Ohtsu, "Local field observation of optical properties on quantum nano-structures using near-field scanning optical microscopy", Technical Report of IEICE (The Institute of Electronics, Information and Communication Engineers), LQE96-85, pp.49-54 (1996). (in Japanese)

10) L. Finger, T. Arakawa, and Y. Arakawa, "PLE Properties of Quantum Wires Fabricated by MOCVD Selective Growth", to be presented in the 44th Spring Meeting, 1997; The Japan Society of Applied Physics and Related Societies.

11) Y. Toda, T. Arakawa, S. Shinomori, and Y. Arakawa, "Observation of Near-Field PL Spectra on Quantum Wires by MOCVD Selective Growth", Fabricated by MOCVD Selective Growth", to be presented in the 44th Spring Meeting, 1997; The Japan Society of Applied Physics and Related Societies.

4 Domestic Conferences (presented in Japanese) Related to Other Works

12) Y. Kato, M. Kitamura, T. Arakawa, T. Tanaka, M. Nishioka, and Y. Arakawa, "Effect of electric field on optical properties of InGaAs quantum dots", The 43rd Spring Meeting, 1996; The Japan Society of Applied Physics and Related Societies, Saitama, March 1996.

13) R. Schur, M. Nishioka, M. Kitamura, T. Arakawa, and Y. Arakawa, "A New Technique for the Fabrication of Self-Organized InGaAs Quantum-Dots by MOCVD", The 43rd Spring Meeting, 1996; The Japan Society of Applied Physics and Related Societies, Saitama, March 1996.